

A Dual Concentration-Tailored Cytokine-Chemo Nanosystem to Alleviate Multidrug Resistance and Redirect Balance of Cancer Proliferation and Apoptosis

Yu Hsia^{1,2}, Maharajan Sivasubramanian¹, Chia-Hui Chu¹, Yao-Chen Chuang^{1,3}, Yiu-Kay Lai², Leu-Wei Lo¹ 

¹Institute of Biomedical Engineering and Nanomedicine, National Health Research Institutes, Zhunan, Taiwan; ²Institute of Biotechnology, National Tsing Hua University, Hsinchu, Taiwan; ³Department of Radiation Oncology, Taipei Medical University Hospital, Taipei, Taiwan

Correspondence: Leu-Wei Lo, Institute of Biomedical Engineering and Nanomedicine, National Health Research Institutes, 35, Keyan Road, Zhunan Town, Miaoli County 350, Zhunan, Taiwan, Tel +886-37-206-166 Ext 37115, Fax +886-37-586-440, Email lwlo@nhri.edu.tw; Yiu-Kay Lai, Institute of Biotechnology, National Tsing Hua University, No. 101, Section 2, Kuang-Fu Road, Hsinchu, 300044, Taiwan, Tel +866-35-742-745, Email lslyk@life.nthu.edu.tw

Background: Cancer multidrug resistance (MDR) is an important factor that severely affects the chemotherapeutic efficacy. Among various methods to bypass MDR, usage of cytokines, such as tumor necrosis factor alpha (TNF α) is attractive, which exerts antitumor effects of immunotherapeutic response and apoptotic/proinflammatory pathways. Nevertheless, the challenges remain how to implement targeted delivery of TNF α to reduce toxicity and manifest the involved signaling mechanism that subdues MDR.

Methods: We synthesized a multifunctional nanosystem, in which TNF α covalently bound to doxorubicin (Dox)-loaded pH-responsive mesoporous silica nanoparticles (MSN) through bi-functional polyethylene glycol (TNF α -PEG-MSN-Hydrazone-Dox) as a robust design to overcome MDR.

Results: The salient features of this nanoplatform are: 1) by judicious tailoring of TNF α concentration conjugated on MSN, we observed it could lead to a contrary effect of either proliferation or suppression of tumor growth; 2) the MSN-TNF α at higher concentration serves multiple functions, besides tumor targeting and inducer of apoptosis through extrinsic pathway, it inhibits the expression level of p-glycoprotein (P-gp), a cell membrane protein that functions as a drug efflux pump; 3) the enormous surface area of MSN provides for TNF α functionalization, and the nanochannels accommodate chemotherapeutics, Dox; 4) targeted intracellular release of Dox through the pH-dependent cleavage of hydrazone bonds induces apoptosis by the specific intrinsic pathway; and 5) TNF α -PEG-MSN-Hydrazone-Dox (MSN-Dox-TNF α) could infiltrate deep into the 3D spheroid tumor model through disintegration of tight junction proteins. When administered intratumorally in a Dox-resistant mouse tumor model, MSN-Dox-TNF α exhibited a synergistic therapeutic effect through the collective performances of TNF α and Dox.

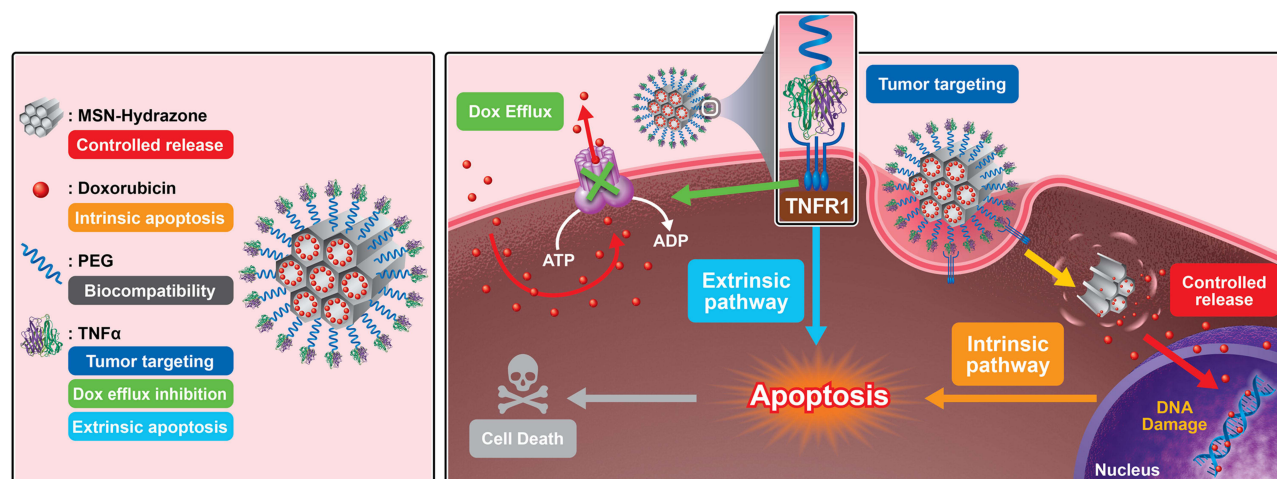
Conclusion: We hereby develop and demonstrate a multifunctional MSN-Dox-TNF α system with concentration-tailored TNF α that can abrogate the drug resistance mechanism, and significantly inhibit the tumor growth through both intrinsic and extrinsic apoptosis pathways, thus making it a highly potential nanomedicine translated in the treatment of MDR tumors.

Keywords: cytokine cancer therapy, tumor necrosis factor alpha, mesoporous silica nanoparticle, pH-responsive controlled release, intrinsic/extrinsic apoptosis pathways, cancer multidrug resistance

Introduction

It is well known that cytokines have been used for cancer therapy. However, their clinical application is held in check due to their unpleasant side effects and expeditious onset of undesired regulatory mechanisms.^{1,2} Knowledge gathered from research shows that these limitations could be overcome by targeted delivery of low-dose cytokines to tumors.³⁻⁵ This could be materialized by conjugating cytokines to targeted tumor cells. For its multifaceted anti-tumor effects, tumor necrosis factor-alpha (TNF α) has been the focus of much attention, including its ability to disintegrate tumor cells, stimulate an immune response against tumors, and activate apoptotic and pro-inflammatory pathways.^{6,7} TNF α is

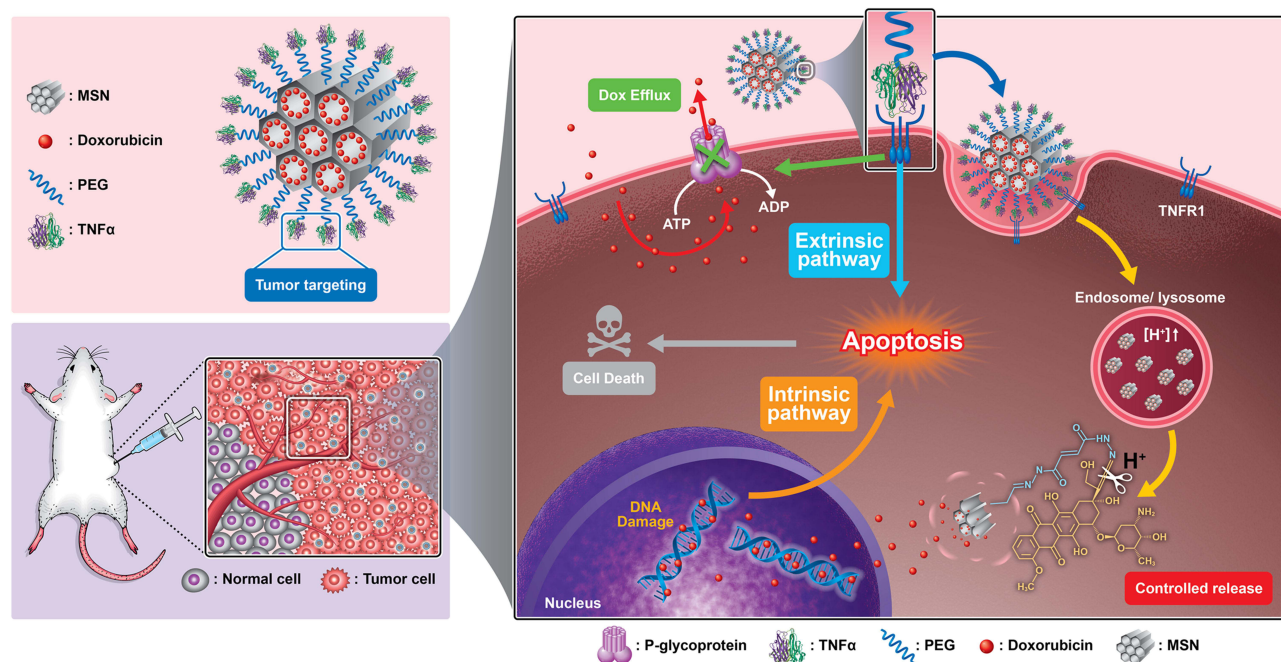
Graphical Abstract



a pleiotropic inflammatory cytokine, which is generally synthesized by natural killer (NK) cells, T lymphocytes, and activated macrophages. TNF α triggers cell inflammation, cell survival, apoptosis, and immunity via two receptors – TNF receptor type 1; p55 (TNFR1) and TNF receptor type 2; p75 (TNFR2).⁸ Therefore, TNFR1 is a significant member of the death receptor family that shares the ability of evoking apoptosis.^{9,10} When TNFR1 signals apoptosis, FADD binds procaspase 8, activating the latter. This activation initiates a protease caspase, causing apoptosis. It also involves mitochondria and caspase as foremost regulators,¹⁰ such as BAK and BAX, which trigger pore formation in the mitochondria causing the formation of apoptosome, then activation of caspase-9 to stimulate the caspase cascade, and final activation of caspase-3/-7.¹¹

TNF α has been studied as an antitumor agent via different routes of administration. Intramuscular and subcutaneous administration of TNF α were already executed, but discontinued due to side effects at the location of injection.^{12,13} Therefore, targeted tumor delivery of TNF α is necessary. Delivery of TNF α using a liposomal delivery platform has shown some potential in animal cancer models, although extremely high dose of the drug is required.^{14,15} Recently, nanoparticles (NP) bound with TNF α may passively accumulate within tumors via either the enhanced permeability and retention (EPR) effect, or active targeting mechanism through an interaction between TNF α and TNFR1. Several publications showed that combination of TNF α with various therapeutic modalities. For example, chemotherapy, radiation and focal thermal therapies have demonstrated better therapeutic efficacy and some of these approaches are being clinically investigated.¹⁶ AurimuneTM (CYT-6091,) (CytImmune Sciences, U.S.A.), a nanoformulation is currently undergoing clinical trials (phase I) as a monotherapy for the treatment of advanced solid tumors.¹⁷ To fabricate CYT-6091, TNF α and a thiol-derivatized polyethylene glycol are chemically attached onto the surface of 33 nm colloidal gold. CYT-6091 delivers TNF α to solid tumors through both active and passive targeting mechanisms.¹⁸ And the photothermal activation of Au-TNF with a laser (approved for medical use which open new approaches in the enlargement of clinically related NP) exhibited a synergistic antitumor therapeutic effect.¹⁹ TNF α not only performs antitumor theranostic action but also serves as potential therapeutics in cerebral ischemia/reperfusion injury. Polymers were also used as a carrier of TNF α . For example, TNF α was loaded in PEG-b-(PELG-g-PLL), the block copolymer released TNF α in a sustained fashion. As a result, better half-life was achieved with enhanced bioactivity.²⁰

Mesoporous silica nanoparticles (MSN) has found critical applications in biology. For example, when a dye molecule is attached to MSN, it could serve as a fluorescent tracker (both in vivo and in vitro),²¹ medical diagnosis,^{22,23} and drug²⁴ and gene delivery.²⁵ MSN offer several advantages over traditional nanomaterials to overcome multidrug resistance (MDR), which can enhance cellular uptake efficacy and increase intracellular drug concentration.²⁶ MSN also possess a passive



Scheme 1 Schematic illustration of construction of MSN-Dox-TNF α that down-regulates the expression of P-gp, facilitating targeted uptake in drug-resistant cancer cells. Intracellular release of Dox through cleavage of hydrazone bonds results in abundant accumulation, which significantly reduces cell viability through both intrinsic and extrinsic apoptosis pathways.

Abbreviations: MSN, mesoporous silica nanoparticles; PEG, polyethylene glycol; Dox, doxorubicin; TNF α , tumor necrosis factor alpha; TNFR1, TNF receptor type I.

targeting function, and majorly accumulate in the tumor via the EPR effect.²⁷ The combination of both active and passive targeting is accomplished by surface modification of MSN with homing molecules, such as peptides, proteins, antibodies, or specific ligands. These “magic bullet” drug delivery platforms depend on the ability of the homing molecules to bind receptors selectively to the cell surface through ligand–receptor interactions.⁶ Previous studies reported the functionalization of MSN with anti-HER2/neu monoclonal antibody (mAb) for specific targeting of breast cancer cells.²⁸

In this study, we developed a TNF α -bound pH-responsive MSN capable of releasing doxorubicin (Dox) intracellularly. TNF α provides tumor-targeting functions and was able to down-regulate the expression of p-glycoprotein (P-gp) to reduce drug resistance. In vivo, the nanoplatform induced a synergistic therapeutic effect through the activation of both extrinsic and intrinsic apoptosis pathways (Scheme 1). It was also determined that the concentration of TNF α is a crucial factor for tumors to undergo either proliferation or apoptosis, two contrary pathways.

Materials and Methods

Experimental Reagent

Dox hydrochloride, bovine serum albumin, adipic acid dihydrazide, paraformaldehyde, phosphate buffer saline (PBS, 0.1 M, pH 7.4), dichloromethane, methanol and acetic acid were purchased from Sigma-Aldrich. Tetraethoxysilane (TEOS), cetyltrimethylammonium bromide (CTAB), ethanol, ammonium hydroxide (30%) and 3-Aminopropyltrimethoxysilane (APTS) were purchased from Acros. n-Octane was purchased from Alfa Aesar. Silane-PEG-Maleimide (M.W. 2000) was purchased from Nanocs Inc. Recombinant Human TNF α protein was purchased from PeproTech Inc. McCoy’s 5A medium, DMEM medium, fetal bovine serum (FBS) and Trypsin-2.5% (W/V) EDTA solution (10X) were purchased from Gibco Co.

Cell Line

Human glioblastoma U87MG cell line was obtained from the Bioresource Collection and Research Center (BCRC). Human uterine sarcoma MES-SA and Dox-resistant MES-SA/Dx5 cell lines were obtained from the BCRC, Taiwan. The MDR cell line was maintained in McCoy’s 5A medium containing 1.5 mM L-glutamine supplemented with 10% FBS in

a humidified incubator at 37°C in an atmosphere of 5% CO₂. The U87MG cell line was maintained in completed DMEM medium.

In vitro Release Study

Dox release from the NP was investigated using appropriate buffer solutions with pH ranging from 7.4 to 1.0. Typically, 20 mg of MSN-Hydrazone-Dox or TNF α -PEG-MSN-Hydrazone-Dox (MSN-Dox-TNF α) was mixed with buffer solution (5 mL) in a falcon tube and placed in a water bath (37°C) and stirred constantly at 100 rpm. Release media were collected for further concentration measurement at specific timepoints by centrifuging at 12,000 rpm for 20 min. The solid NP pellets were resuspended with 5 mL of fresh buffer solution. The amount of Dox released from the solid NP was determined by measuring the absorbance at 485 nm.

ELISA Assay

To determine TNF α concentration in MSN-Dox-TNF α or MSN-TNF α quantitatively, an ELISA kit from Abcam was used. The standard, sample, or control was added to each of the 96-well plates coated with monoclonal antibodies with specificity for human TNF α , and incubated for 2 h at room temperature. Following the manufacturer's protocol, the 96-well plates were washed four times with a wash buffer. The assay plates were sequentially incubated with polyclonal horseradish peroxidase (HRP)-conjugated anti-TNF α antibodies for 1 h at room temperature. Each well was aspirated and washed four times. The assay plates were developed using 3,3',5,5' tetramethylbenzidine (TMB) and a hydrogen peroxide (H₂O₂) solution in darkness. Absorbance was determined by using an ELISA reader, measuring the absorbance at 450 nm and a reference absorbance at 540 or 570 nm.

Cell Viability via MTT

3-(4,5-dimethylthiazol-2-yl)-2,5-diphenyltetrazolium bromide (MTT) assay was applied to evaluate the cytotoxicity of MES-SA/Dx5 and MES-SA cell lines treated with various formulations. The cells were treated with 5 or 0.4 μ g/mL free Dox, 100 ng/mL free TNF α , 50 μ g/mL PEG-MSN, PEG-MSN-Hydrazone-Dox (MSN-Dox) (containing a Dox-equivalent dose of 0.40 μ g/mL), TNF α -PEG-MSN (MSN-TNF α), and MSN-Dox-TNF α (containing a Dox-equivalent dose at 0.40 μ g/mL) for 24 to 72 h. Each free drug or NP was treated in triplicate. Cytotoxicity was evaluated via MTT assay, in which 10 μ L of an MTT (5 mg/mL) solution and 90 μ L of completed medium mixture was added to each well and incubated for another 4 h. Then, the medium was removed, followed by the addition of 100 μ L DMSO. Absorbance was determined by ELISA reader, measuring the absorbance at 570 nm.

Confocal Microscopy

To monitor the intracellular uptake and localization of NP on MES-SA/Dx5 cells. 5 \times 10⁴ MES-SA/Dx5 cells were seeded onto 35-mm ibidi dishes in a humidified incubator at 37°C in an atmosphere of 5% CO₂ overnight. The cells were treated with 50 μ g/mL NP in a serum-free medium incubated in a humidified incubator for 6 hours. The cells were washed 3 times with PBS to remove the free NP and changed to completed medium. At specific timepoint, the cells were stained with Hoechst 33,342 and 1 mmol/L of LysoTracker Green DND-26 for 20 minutes. Then, the cells washed 3 times with PBS, and changed to serum-free medium for further optical live cell imaging observation. Images of the cells were monitored on a LEICA TCS SPE confocal imaging system with fluorescence observed at excitation wavelengths of 350, 488, 504, and 647 nm. Antibodies for confocal microscopy: ZO-1 (GTX108613, 1:500), Ki-67 (GTX82777, 1:500), Rabbit IgG Dylight488 (GTX213110-04, 1:1000), Mouse IgG DyLight594 (GTX213111-05, 1:1000).

Membrane Protein Extraction and Western Blot

Following the manufacturer's protocol, the membrane proteins were extracted from MES-SA/Dx5 cells using the compartmental protein extraction kit (Chemicon Inc.). In caspase-related analysis, the treated cells were lysed with ice-cold RIPA lysis buffer complemented with protease and phosphatase inhibitor cocktail for 30 min on ice and collected the supernatant by centrifuging at 12,000 rpm for 20 min at 4 °C. The concentration of protein was measured by BCA assay (Thermo Fisher Scientific) and an equal amount of protein lysates was electrophoresed on an 8–15%

polyacrylamide gel at 25 mA for 2–3 h based on the level of separation. The proteins were transferred to methanol pre-soaked polyvinylidene difluoride (PVDF) membrane (0.2 µm pore size) through wet blotting at 250 mA for 2 h (in cold room) (Biorad, Billerica, MA, USA). Blocking was performed using 3–5% BSA in 1x PBS-T (1X PBS 0.1% TWEEN-20) for 1 h at RT, and then the membrane was incubated with primary antibodies at 4 °C overnight. Then, the membrane was washed 4 times with 1x PBS-T to remove unbound antibody, and the membrane were incubated with secondary antibody HRP-goat-anti-rabbit/mouse (1:1000) for 1 h at RT. Then, a washing process was performed with 1X PBS-T and developed using a femto chemiluminescent substrate (Thermo Scientific) and the image analysis was carried out using ImageJ software. Antibodies for Western blotting: P-gp (GTX108370, 1:500), Caspase-3 (GTX110543, 1:1000), Caspase-8 (GTX110723, 1:1000), Caspase-9 (GTX22324, 1:1000), β actin (GTX109639, 1:5000).

Caspase Multiplex Activity Assay

Caspase-3, caspase-8 and caspase-9 Multiplex Activity Assay Kit (Fluorometric) (Abcam, ab219915) provide a tool to quantify caspase-3, -8, -9 activity in cells that are undergoing apoptosis. This kit uses DEVO-ProRed, IETD-R110 and LEHD-AMC as fluorogenic indicators for caspase-3, -8, -9 activity respectively. Upon caspase cleavage, three distinct fluorophores are released, which can be readily monitored according to the manufacturer's instructions.

Analysis of Uptake of Dox by Flow Cytometry

MES-SA or MES-SA/Dx5 cells were collected from the free Dox or different NP treatment condition. Cells were fixed and washed three times with PBS. The cell lysate was resuspended and stored in 1 mL PBS at 4 °C. FLOW cytometric analysis was performed by using the FACSCalibur flow cytometer with an excitation wavelength of 488 nm and an emission wavelength of 590 nm (FL2). To monitor and quantify the uptake amount of Dox at different treatment conditions.

3D Spheroids Model Assay

The 3D spheroid model mimics in vivo tumor matrix and is used to examining NP penetration and Dox uptake of U87MG cells. 3D cell spheroids were prepared by following steps: 100 µL melted agarose gel (2%) was added to each well of a 96-well plate and cooled down to RT. 100 µL of completed medium (DMEM with 5% fetal bovine serum) containing 5000 u87MG cells were seeded and were incubated in a 5% CO₂ humidified incubator at 37 °C for 3–5 d. Spheroids were treated with free Dox (0.4 or 5 µg/mL) or 50 µg/mL different NP for up to 24 h, then washed 3 times with PBS to remove the free NP and changed to completed medium. At 24 and 48 h spheroids were fixed. Only sections of the middle of spheroids were visualized to exclude NP or free drug adhering to the surface of the spheroids. 3D spheroid sections were mounted onto glass slides and imaged using confocal microscopy to monitor the Dox distribution and cell–cell tight junction leakage by Zonula occludens-1 (ZO-1) staining.

Animal Model

All animal procedures were performed in accordance with the Guidelines for Care and Use of Laboratory Animal of the National Health Research Institutes, Taiwan, and approved by the Institutional Animal Care and Use Committee of National Health Research Institutes, Taiwan (NHRI-IACUC-105110). Four- to six-week-old male nude mice (nu/nu) were purchased from the BioLASCO Taiwan Co. MES-SA/Dx5 cells ($5 \times 10^6/100 \mu\text{L}$) in PBS was mixed with the same volume of BD Matrigel and was subcutaneously injected into the right flank of the mice. The mice were randomly assigned to different treatment groups and administered intratumorally, volume of the tumor used in this study was 100 mm³. The treatment groups consist of a control (treated with PBS), free Dox (0.4 µg/mL), TNFα (100 ng/mL), vehicle control (PEG-MSN), MSN-Dox, MSN-TNFα, and MSN-Dox-TNFα. All NP were administered at a concentration of 50 µg/mL at Day 0, and tumor growth and body weight were measured every 3 or 4 days. After the experiment was completed, tumors from each treatment groups were harvested and immunostaining was performed.

Statistical Analysis

All data were expressed as the means \pm SEM. The statistical analysis was performed by Student's *t*-test and two-way ANOVA. Statistical significance was set to $\alpha=0.05$.

Results

MSN are Loaded with Dox and TNF α to Generate pH-Controlled Drug Released System

MSN with extended pore size that bore hexagonal structure was prepared in the presence of CTAB, a pore expanding agent in alkaline condition. After the sol-gel co-condensation reaction, CTAB was extracted under NH₄NO₃-alcohol mixture for further conjugation.

The conjugation of the pH-sensitive linker onto the MSN nanochannel involves two steps. Step 1: modification of the MSN inner and outer surface with an aldehyde group using triethoxysilylbutyraldehyde. Step 2: The aldehyde group was subsequently reacted with adipic acid dihydrazide to generate a pH-reactive hydrazone bond. In addition, another hydrazide group was further reacted with the ketone group of Dox to establish additional hydrazone bonds in Dox. Therefore, the as-synthesized pH-sensitive MSN with two hydrazine bonds, when loaded with the drug, could be cleaved and release the drug in an acidic environment. The amount of Dox loaded in MSN was evaluated by UV-Vis spectrophotometer. The amount of Dox loaded in MSN-Hydrazone was 0.85%, respectively.

Finally, the pH-sensitive MSN outer surface was engineered with hetero-functional polyethylene glycol and TNF α . First, a bi-functional PEG coating silane and maleimide groups were attached to the MSN outer surface. Followed by the reaction with the sulfhydryl groups of TNF α at pH 7.2 to form stable thioether bonds, resulting in MSN-Dox-TNF α .

The size of NP has a strong correlation with their in vivo clearance routes. For example, NP with a diameter of 3 nm or less will extravasate tissues in a non-specific manner, whereas NP with diameters less than 6 nm will undergo renal filtration. It well known that NP with sizes ranging from 30 to 80 nm tend to accumulate in the lungs as well as in areas with leaky vasculature. Large-sized NP (>80 nm) exhibit an increased tendency to be trapped by mononuclear phagocyte system. Accordingly, our synthesized MSN size was less than 80 nm in diameter in order to reduce hepatic accumulation and increase tumor targeting. TEM images of MSN and MSN-Dox are shown in Figure 1a. Using n-octane as a swelling agent, our synthesized MSN had a large pore diameter (~4.0 nm). Figure 1b shows the Fourier transform infrared (FTIR) analysis of MSN, Dox, PEG and MSN-Dox-TNF α evidenced features unique to all of them. PEG and MSN-Dox-TNF α show characteristic stretching frequencies for C-O at 1080 cm⁻¹. Dox and MSN-Dox-TNF α both provided characteristic stretching frequencies for C=C ring structure at 1617, 1582, 1414 cm⁻¹. But the TNF α as a protein is difficult to be analyzed by FTIR analysis, so we use the specific ELISA kit form Abcam to determine the TNF α concentration in MSN-Dox-TNF α or MSN-TNF α quantitatively. As shown in the figure, MSN has uniform sizes and hexagonal shapes, with an average particle diameter of approximately 62 \pm 6.8 ~ 75 \pm 4.9 nm (Figure 1c). The surface charge of synthesized MSN, MSN-Dox, or MSN-Dox-TNF α were determined by zeta-potential measurements. Bare MSN and MSN-Dox showed a strong negative zeta potential due to the presence of surface silanol groups, while MSN-Dox-TNF α showed a slight reduction in zeta potential due to the surface coverage by TNF α . Polydispersity (PDI) index is a parameter to define the particle size distribution, the smaller PDI denotes that nanoparticles are more homogeneous. The PDI values of nanoparticles ranging from 0.01 to 0.5–0.7 possess good dispersibility and stability. PDI values bigger than 0.7 indicate that the sample has a very broad particle size distribution. The PDI of MSN, MSN-Dox and MSN-Dox-TNF α were found to be 0.072 \pm 0.007, 0.075 \pm 0.01 and 0.174 \pm 0.08 respectively. These NP show highly colloidal stability due to their low PDI values.

To evaluate the pH-responsive behavior of our nanopatform (Figure 1d), we performed in vitro Dox release studies under various pH (7.4, 5.5, 4.5, and 1.0). The drug-releasing experiment was carried out with PEG-MSN-Hydrazone-Dox (denoted as MSN-Dox) and MSN-Dox-TNF α . For MSN-Dox at pH 1.0, a burst release of Dox was observed at earlier time points, at which ~72.7% of Dox was released in 6 h. This might be due to the co-operative accelerated degradation of hydrazine bonds and protonation of amine groups that resulted in complete Dox release in 120 h. However, at pH 4.5 and 5.5, smaller burst release patterns were observed, resulting in ~42.8% and ~26.7% of Dox release in 6 h; at 120 h, the

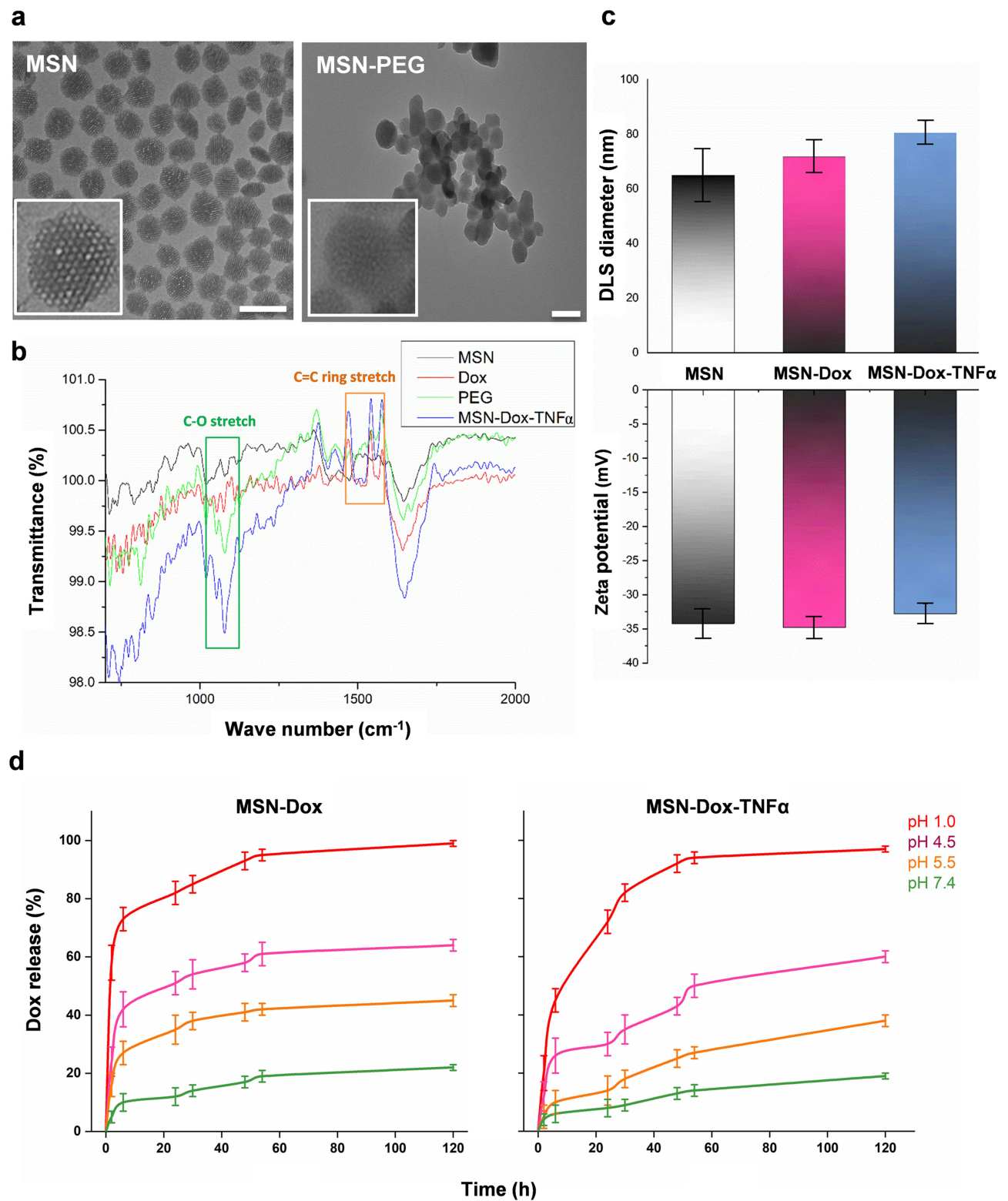


Figure 1 Characterization of the synthesized nanomaterials. (a) TEM photos of MSN and MSN-PEG. Scale bars: 100 nm. (b) FTIR spectra of MSN, Dox, PEG and MSN-Dox-TNF α . (c) DLS diameter and zeta potential changes after functionalization. (d) Dox release profiles at various pH values.

Abbreviations: MSN, mesoporous silica nanoparticles; PEG, polyethylene glycol; Dox, doxorubicin; TNF α , tumor necrosis factor alpha; MSN-Dox, PEG-MSN-Hydrazone-Dox; MSN-Dox-TNF α , TNF α -PEG-MSN-Hydrazone-Dox.

Dox release from pH 4.5 and 5.5 were 62.3% and 41.8%, respectively. In MSN-Dox-TNF α , the burst release of Dox (~44.7% in 6 h) at pH 1.0 was decreased compared to MSN-Dox; however, Dox was completely released in 120 h. Similarly, MSN-Dox-TNF α in pH 4.5 and 5.5 showed reduced burst release patterns compared to MSN-Dox. A plausible reason for this might be the presence of TNF α offering steric hindrance to Dox release. Irrespective of the samples, ie, either MSN-Dox or MSN-Dox-TNF α at pH 7.4, Dox release was minimal; and at 120 h, Dox release from both samples was less than 20%. It indicates the robust pH-responsive nature of our developed nanoplatform.

In vitro Cellular Uptake in MDR Cells

To study the uptake behavior and intracellular distribution of MSN-Dox and MSN-Dox-TNF α , Dox fluorescence was observed using a confocal microscope (Figure 2). Followed by the incubation for 2 h, MSN-Dox and MSN-Dox-TNF α was found to be co-localized (red fluorescence) within lysosome (green fluorescence). MSN-Dox-TNF α treated cells showed strong fluorescence signal compared to MSN-Dox. This might be attributable to the reduced expression of P-gp by TNF α that weakened the drug resistance mechanism. As a result, at 24 h post-incubation, the released Dox from the NP was able to co-localize in the nucleus. These results showed that TNF α plays a dual role as a targeting agent and attenuated drug resistance mechanism that helped Dox to accumulate in high concentrations within lysosomes followed by transition to the nuclei of MES-SA/Dx5 cells.

MSN-Dox-TNF α Enhances Cytotoxicity of MES-SA/Dx5 Cells

First, the viability of Dox-resistant and sensitive cells were assessed with MSN only and free Dox. The results showed that, irrespective of the cell lines tested, MSN did not induce toxicity, and cell viability was over 90% in both MES-SA/Dx5 and MES-SA cells (Figure 3a). The synergistic effect of Dox and TNF α was estimated by combination index (CI) analysis, the CI was calculated using the formula $CI = D1/Dm1 + D2/Dm2$, where D1 and D2 are the doses of Dox and TNF α combined to reach the 50% reduction in cell viability and Dm1 and Dm2 are the concentrations of the single treatment to reach the same effect. The CI values provide quantitative definition for synergism (CI<1), additive effect (CI=1) or antagonism (CI>1). For this purpose, MES-SA/Dx5 cells after different treatment were analyzed with MTT assay (Figure 3b) to monitor the half maximal inhibitory concentration (IC₅₀). The CI of Dox and TNF α is calculated to be around 0.8, verifying the synergistic effect. When treated with Dox (5 μ g/mL), however, the viability of MES-SA cells was significantly reduced to 10% at 72 h. Moreover, at the same condition, the viability of MES-SA/Dx5 cells at 72 h was ~70%, which indicates a drug-resistant nature. Then, using MES-SA/Dx5 cells, we performed the cell viability test using various formulations, including free Dox, MSN-Dox, MSN-TNF α , and MSN-Dox-TNF α . From these results (Figure 3c), it could be seen that MSN-Dox-TNF α significantly reduced cell viability compared to free Dox at an equivalent dose. MSN-Dox-TNF α decreased cell viability to less than 50% compared to the control at 24 h. Furthermore, when the experiment time was extended to 48 h and 72 h, cell viability was decreased to 20% and 10% compared to the control, respectively. Compared to the results from Figure 3b, even though the concentrations of Dox and TNF α loaded in MSN-Dox-TNF α were low. The co-delivery of Dox and TNF α from MSN-Dox-TNF α provided better cell-killing efficacy than free Dox and TNF α at the same time point. This result shows that the combination of TNF α and Dox induced synergistic cell-killing ability in Dox-resistant cells. The mechanism of antitumor enhancement might be contributed by intrinsic and extrinsic apoptosis pathways of Dox and TNF α .

Caspase Activity Analysis of Expression Levels of Apoptotic Protein by MDR Cells Treated with Different NP

To clarify the mechanism underlying the effects of NP treatment-induced apoptosis, we investigated protein expression associated with apoptosis in MES-SA/Dx5 cells. The two main pathways of apoptosis are intrinsic and extrinsic pathways. Specific signaling is required for each pathway to initiate a series of molecular events. Intrinsic apoptosis is triggered by cellular stress, which results in the activation of the Bcl-2 family of proteins. On the other hand, the extrinsic apoptosis pathway is activated when ligands bind to their corresponding death receptors and recruit FADD to these receptors. Each pathway activates its own initiator caspase-8 or caspase-9, and triggers the major executioner caspase-3. As shown in

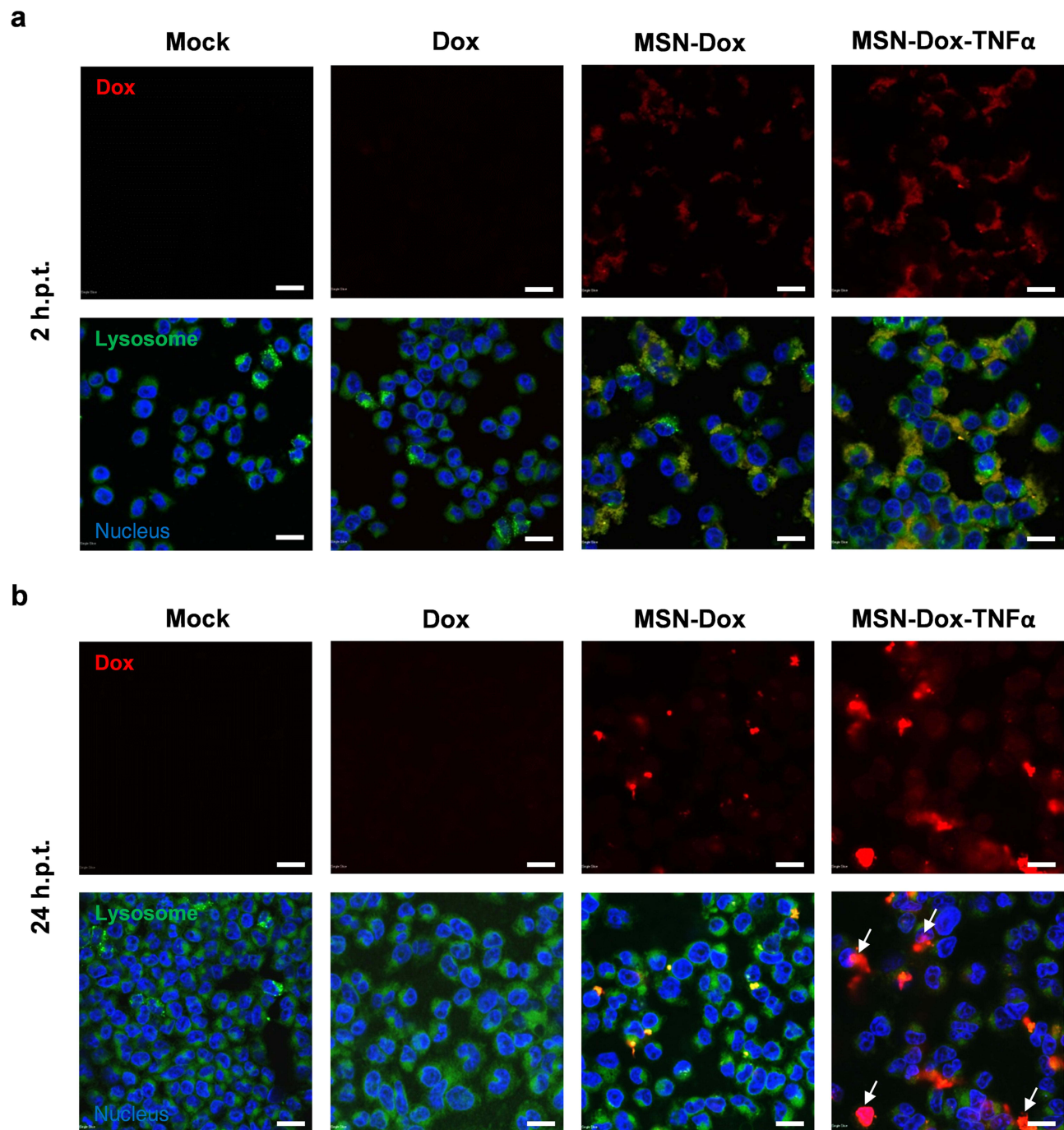


Figure 2 In vitro cellular uptake of free Dox, MSN-Dox, or MSN-Dox-TNF α at various time points were visualized by confocal microscopy in MES-SA/Dx5 cells incubation time (a) 2 h and (b) 24 h with 50 $\mu\text{g}/\text{mL}$ NP or 0.4 $\mu\text{g}/\text{mL}$ Dox. Dox showed red fluorescence. Lysosomes stained with lysotracker green probe. Nucleus was stained by DAPI. Note the higher level of MSN-Dox-TNF α uptake, and the colocalization of the MSN within the lysosomes. Colocalization of Dox within the nucleus (indicated by white arrow) after 24 h post-treatment. Scale bars: 20 μm .

Abbreviations: MSN, mesoporous silica nanoparticles; Dox, doxorubicin; TNF α , tumor necrosis factor alpha; MSN-Dox, PEG-MSN-Hydrazone-Dox; MSN-Dox-TNF α , TNF α -PEG-MSN-Hydrazone-Dox; h.p.t., hours post-treatment.

Figure 4a, Dox-loading NP (MSN-Dox and MSN-Dox-TNF α) triggered the intrinsic apoptosis pathway, and enhanced the activated caspase-9 and caspase-3 expression. Activation of the extrinsic type I signaling pathway, which involves direct cleavage and activation of caspase-3 by caspase-8, was observed as a result of using NP conjugates containing TNF α , such as MSN-TNF α or MSN-Dox-TNF α , ultimately leading to apoptosis. Western blot results showed enhanced activated caspase-3 signals and reduced full length caspase-8 (inactivated form) signals in a time-dependent manner. A previous investigation

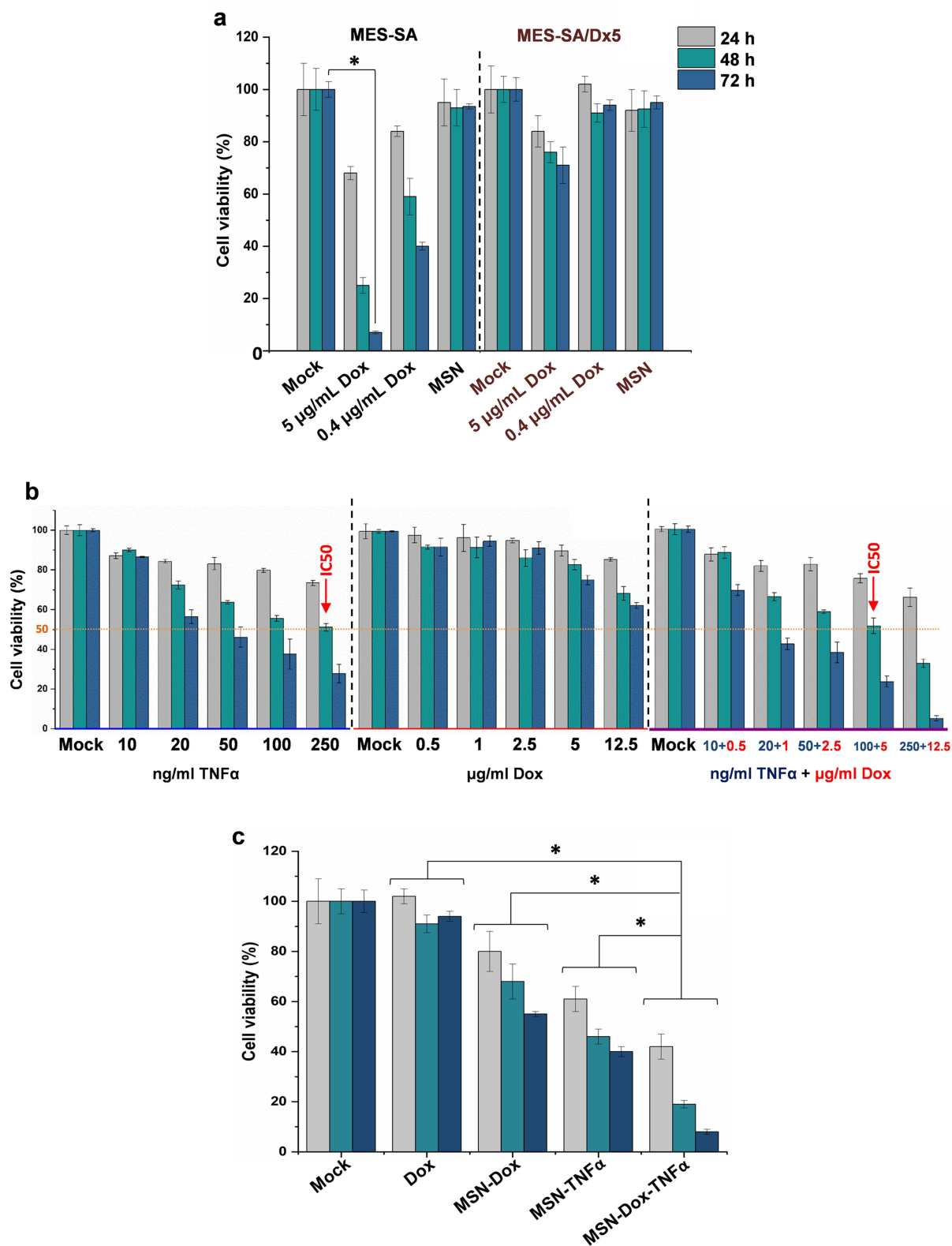


Figure 3 Evaluation of cell viability of MES-SA/Dx5 cells in the presence of different NP. (a) Cytotoxic effects of Dox or MSN on MES-SA or MES-SA/Dx5 seeded with a density of 5×10^4 cells in 100 μ L medium incubated with Dox only (0.4 or 5 μ g/mL) or 50 μ g/mL MSN. Data are the mean \pm SEM expressed as viability percentage relative to mock. * $P < 0.05$ vs mock. (b) Combination treatment with Dox and TNF α on MES-SA/Dx5 cell line. (c) Seeded MES-SA/Dx5 cells were incubated with Dox (0.4 μ g/mL) or different NP (50 μ g/mL). Cell viability was quantified at various time points. Data are the mean \pm SEM expressed as viability percentage relative to mock. * $P < 0.05$ at each time points. **Abbreviations:** Dox, doxorubicin; MSN, mesoporous silica nanoparticles; TNF α , tumor necrosis factor alpha; MSN-Dox, PEG-MSN-Hydrazone-Dox; MSN-TNF α , TNF α -PEG-MSN; MSN-Dox-TNF α , TNF α -PEG-MSN-Hydrazone-Dox.

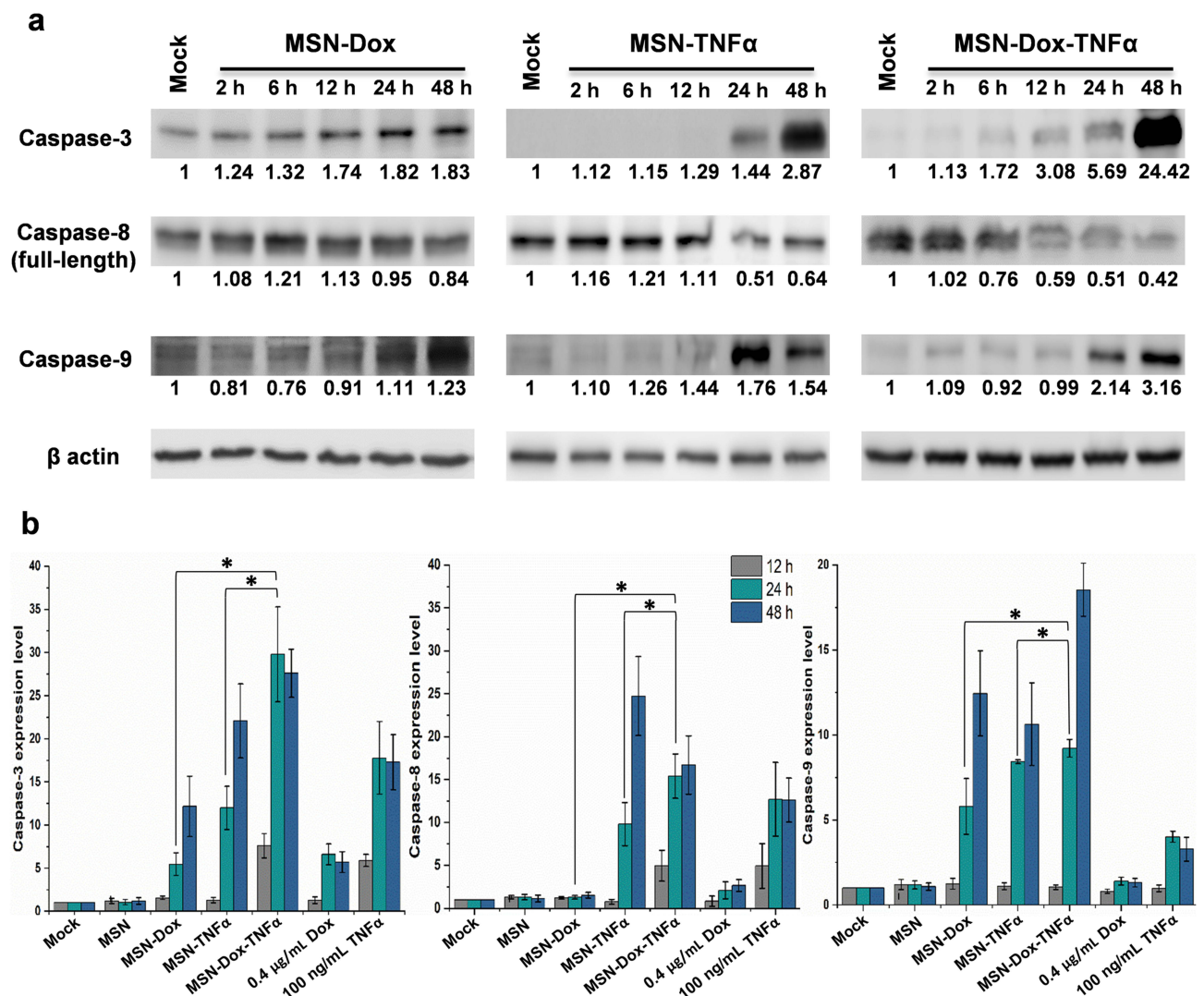


Figure 4 Caspase activity analysis of expression levels of apoptotic protein by MES-SA/Dx5 cells treated with different NP after 2, 6, 12, 24, or 48 h. The level of activated caspase-3, activated caspase-9, or full-length caspase-8 was analyzed by (a) Western blot analysis or (b) multiplex activity assay kit (Abcam). There was an increase of activated caspase-3 and caspase-9, and a decrease of full-length caspase-8, that were obviously more pronounced in the MSN-Dox-TNF α group than the other treatments. Data are the mean \pm SEM expressed as fold-change related to mock. *P<0.05.

Abbreviations: MSN, mesoporous silica nanoparticles; Dox, doxorubicin; TNF α , tumor necrosis factor alpha; MSN-Dox, PEG-MSN-Hydrazone-Dox; MSN-TNF α , TNF α -PEG-MSN; MSN-Dox-TNF α , TNF α -PEG-MSN-Hydrazone-Dox.

reported the extrinsic type II signaling pathway, in which caspase 8 activates BAK and BAX proteins, which induce the intrinsic pathway, causing activated caspase-9 and caspase-3. We confirmed these results by caspase multiplex activity assay (Figure 4b). The results obtained were comparable to those of the Western blot analysis. The results indicated that Dox induced the intrinsic apoptosis pathway and TNF α stimulated the extrinsic apoptosis pathway. MSN-Dox-TNF α treatment triggered both apoptosis pathways, and has the potential to achieve a synergistic therapeutic effect.

Effect of MSN-TNF α on P-Gp Expression in MDR Cells

MDR is a phenomenon exhibited by the tumors to resist chemotherapeutic agents by expressing P-gp is a main causative factor leading to MDR, such as MES-SA/Dx5. TNF α induced a reduction in P-gp expression levels, which leads to a reduced P-gp efflux function. First, we analyzed mRNA and protein expression levels in MES-SA/Dx5 cell lines under MSN-TNF α treatment. Based on our data, MSN-TNF α induced the down-regulation of endogenous P-gp transcript levels in MES-SA/Dx5 cells after 24 h incubation (Figure 5a). P-gp protein levels also decreased in MES-SA/Dx5 cell lines after 24 h incubation compared with the untreated condition (Figure 5b). The main function of P-gp in MDR cells is

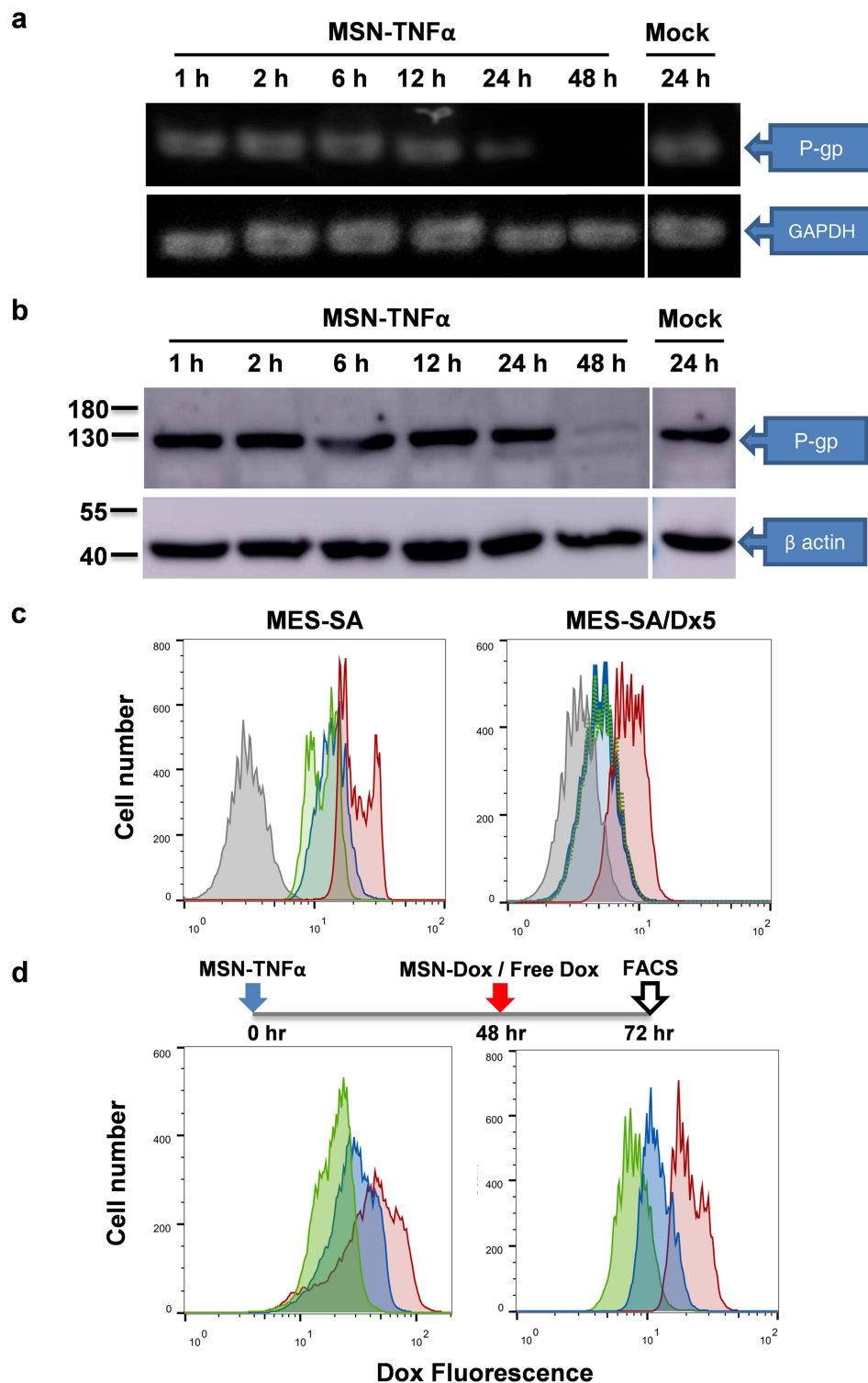


Figure 5 P-gp expression inhibited by MSN-TNF α treatment in MES-SA/Dx5 cells. (a) RT-PCR and (b) Western blot analysis of P-gp expression level. Amplification of GAPDH was used as a control for RT-PCR assays. For loading control in the Western blot assay, the membrane was incubated with anti- β actin antibody. (c) MES-SA (Dox-sensitive) or Dox-resistant counterpart cells were treated with free Dox and analysis of uptake of Dox by flow cytometry. Gray line: mock, red line: free Dox (6 h.p.t.), blue line: free Dox (24 h.p.t.) and green line: free Dox (48 h.p.t.). (d) MSN-TNF α increases tumor cell uptake of Dox by inhibiting P-gp expression. Green line: Free Dox treatment without MSN-TNF α pretreatment, red line: MSN-TNF α 48 h.p.t. then treat with MSN-Dox or free Dox (blue line).

Abbreviations: P-gp, p-glycoprotein; MSN, mesoporous silica nanoparticles; Dox, doxorubicin; TNF α , tumor necrosis factor alpha; MSN-Dox, PEG-MSN-Hydrazone-Dox; MSN-TNF α , TNF α -PEG-MSN; FACS, fluorescence-activated cell sorting.

associated with its membrane pump function, which enables it to eliminate several drugs, such as Dox, out of cancer cells. After observing a reduction in both P-gp mRNA and protein expression levels in MES-SA/Dx5 cell lines following a 48-hour treatment with MSN-TNF α , we proceeded to investigate the effect of MSN-TNF α on P-gp efflux activity in these cells. First, we compared the MES-SA (Dox-sensitive) and MES-SA/Dx5 (Dox-resistant) cells treated with free Dox, and analyzed the uptake efficacy of Dox by flow cytometry (Figure 5c). After 6, 24, and 48 h post free Dox treatment, MES-SA cell samples showed fluorescence peak correspond to a lack of P-gp. The fluorescence of MES-SA/Dx5 cells decreased from 60% (6 h.p.t.) to 15% (24 and 48 h.p.t.) which indicates the P-gp mediated drug resistance mechanism. Next, we treated cells with MSN-TNF α first, and with MSN-Dox or free Dox 48 h later. We then performed 24 h post-treatment analysis of uptake efficacy of Dox by flow cytometry (Figure 5d). The MES-SA cells (with no P-gp expression) showed the same pattern as free Dox without MSN-TNF α pre-treatment. The expression of P-gp was inhibited after MSN-TNF α pre-treatment for 48 h, showed fluorescence peak corresponding to P-gp decrease. Compared to free Dox and MSN-Dox treatments, the latter enriched the Dox concentration than that of free Dox against MES-SA/Dx5. This might be due to the endocytosis of MSN-Dox and controlled release of in the acidic environment, such as endosome/lysosome that locates in the peripheral region of nucleus to preferably bypass the efflux action. TNF α treatment inhibited the P-gp expression, as a consequence, Dox accumulation was increased similar to our MTT assay result, in which MSN-Dox-TNF α combined therapy provides the highest cytotoxicity.

3D Spheroids Model: MSN-Dox-TNF α Distribution and Cell-Cell Tight Junction Leakage

To investigate the deep tumor-penetration ability, we examined the uptake, penetration, and distribution of free Dox, MSN-Dox, and MSN-Dox-TNF α in a 3D tumor spheroids model after 24 h and 48 h treatment. Irrespective of the concentration, free Dox showed little or no uptake in tumor spheroids at 24 h. Moreover, weak Dox signals were observed only at the tumor spheroids periphery at 48 h. MSN-Dox-treated tumor spheroids showed modest Dox fluorescent signals in the tumor periphery at 24 h, and the signals increased slightly at 48 h. MSN-Dox-TNF α -treated tumor spheroids exhibited enhanced uptake, deep penetration, and wide distribution in tumor spheroids. Strong Dox fluorescence signals were observed throughout the tumor spheroids at both 24 h and 48 h. This is because TNF α , as a homing peptide, helped the accumulation of Dox compared to other treatment groups (Figure 6a and b). We wondered whether the deep tumor-penetration ability might be ascribed to the disintegration of tight junction proteins by TNF α , and thus we observed the effect of NP treatments on tight junction proteins. Zonula occludens-1 (ZO-1), which plays a role as a scaffold protein that anchors transmembrane or cytoplasmic proteins, is required for construction of adherents or tight junctions. ZO-1 protein curbs permeability in tight junctions by forming a stabilizing crosslink with these barriers.²⁹ Confocal microscopy images demonstrated that the treatment with MSN-TNF α disrupted ZO-1 content in our 3D spheroids model compared to mock or sonicated cells as a positive control (Figure 7). MSN-Dox-TNF α -treated 3D spheroids significantly abolished the cell barriers. The tight and organized morphology of ZO-1 in the mock was compared with the disrupted and aggregated ZO-1 in response to NP treatment. The MSN-Dox-TNF α treatment significantly enhanced the disruption of ZO-1 localization, which allowed the NP to penetrate deeply into the core of the tumor.

In vivo Antitumor Efficacy of MSN-Dox-TNF α

To observe the tumor growth inhibitory effect, various formulations were intratumorally administered in mice bearing MES-SA/Dx5 tumors. Figure 8a and b shows the changes in tumor volume and body weight of the mice treated with various formulations. Mice were treated with control conditions of free TNF α and MSN only, both showed no therapeutic effect. The tumor volumes continued to increase from days 1 to 24. In the treated concentration of 100 ng/mL, TNF α exhibited no effect on tumor inhibition. In contrast, free Dox and MSN-Dox-treated mice showed a modest tumor inhibition effect. Free Dox has the tendency to diffuse out of the tumor rapidly due to the absence of tumor retention ability. MSN-Dox, on the other hand, possesses the ability to be retained in the tumor and release Dox in a slow manner, and thus a better antitumor effect than Dox only treatment. Among all of the treatment groups, MSN-Dox-TNF α

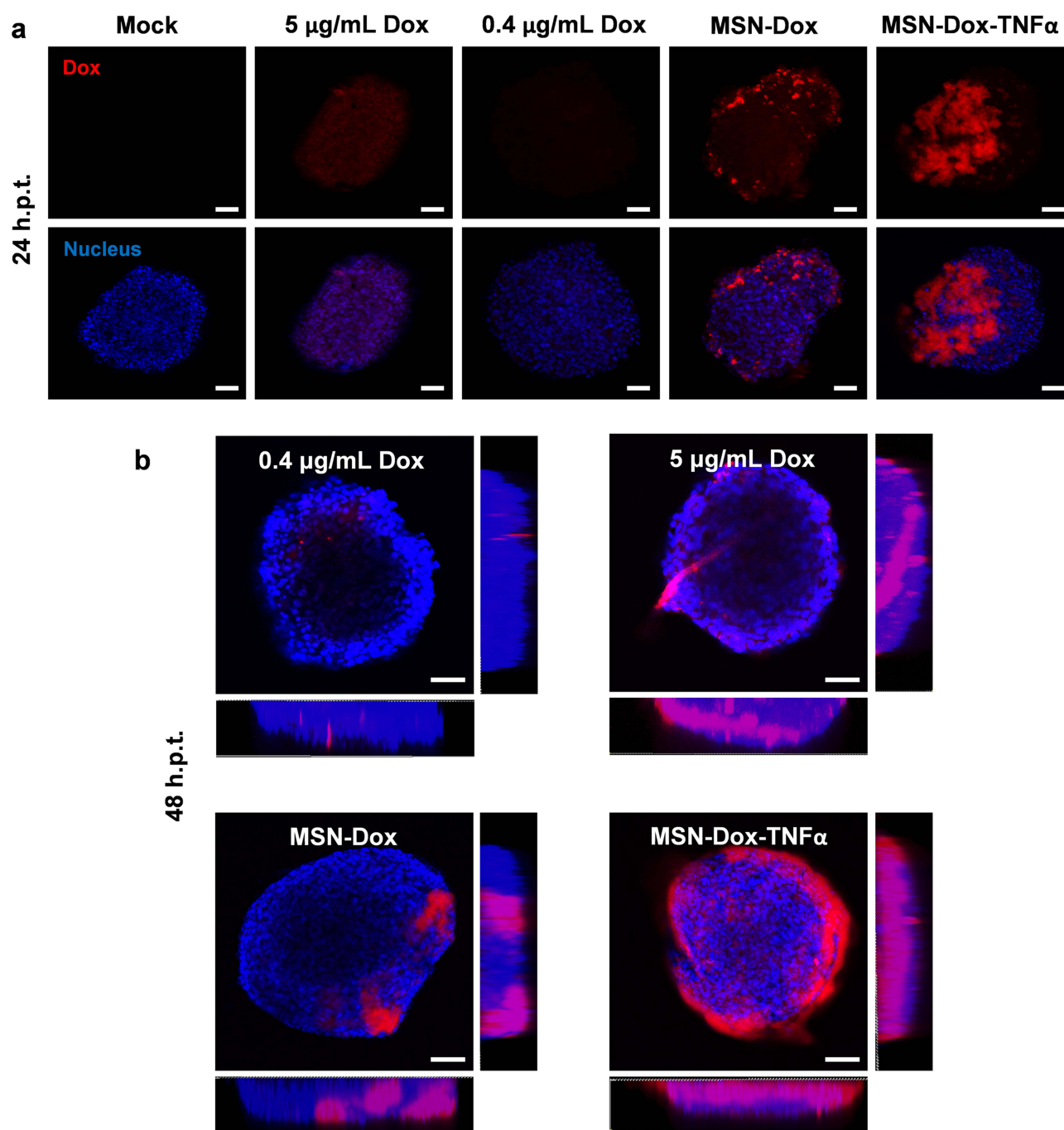


Figure 6 Impact of Dox uptake on MSN-Dox-TNF α treatment in 3D u87MG cell spheroids. U87MG cells were grown as 3D spheroids, and treated with Dox (0.4 or 5 $\mu\text{g/mL}$), MSN-Dox, or MSN-Dox-TNF α . The nuclei were stained by DAPI (blue fluorescence), and red fluorescence signals were from Dox. 3D cell spheroids were fixed at (a) 24 h or (b) 48 h post-treatment. (b) It also shown the images along z-axis to demonstrate the penetration ability of NP. Fluorescence images were obtained with confocal microscopy at the indicated time points. Scale bars: 100 μm .

Abbreviations: MSN, mesoporous silica nanoparticles; Dox, doxorubicin; TNF α , tumor necrosis factor alpha; MSN-Dox, PEG-MSN-Hydrazone-Dox; MSN-Dox-TNF α , TNF α -PEG-MSN-Hydrazone-Dox; h.p.t., hours post-treatment.

demonstrated a significant tumor inhibition effect. The observed tumor growth reduction was due to the combination of Dox and TNF α . It is worth noting that MSN-TNF α -treated mice displayed a contradictory effect, in which MSN-TNF α treatment did not show a tumor inhibition effect, but rather increased the tumor volume after 14 d, implicating the late-phase instigation of tumor proliferation by MSN-TNF α . In addition, there were no significant body weight changes in mice treated with various formulations, which indicates that the treatments had no adverse effects on mice and were

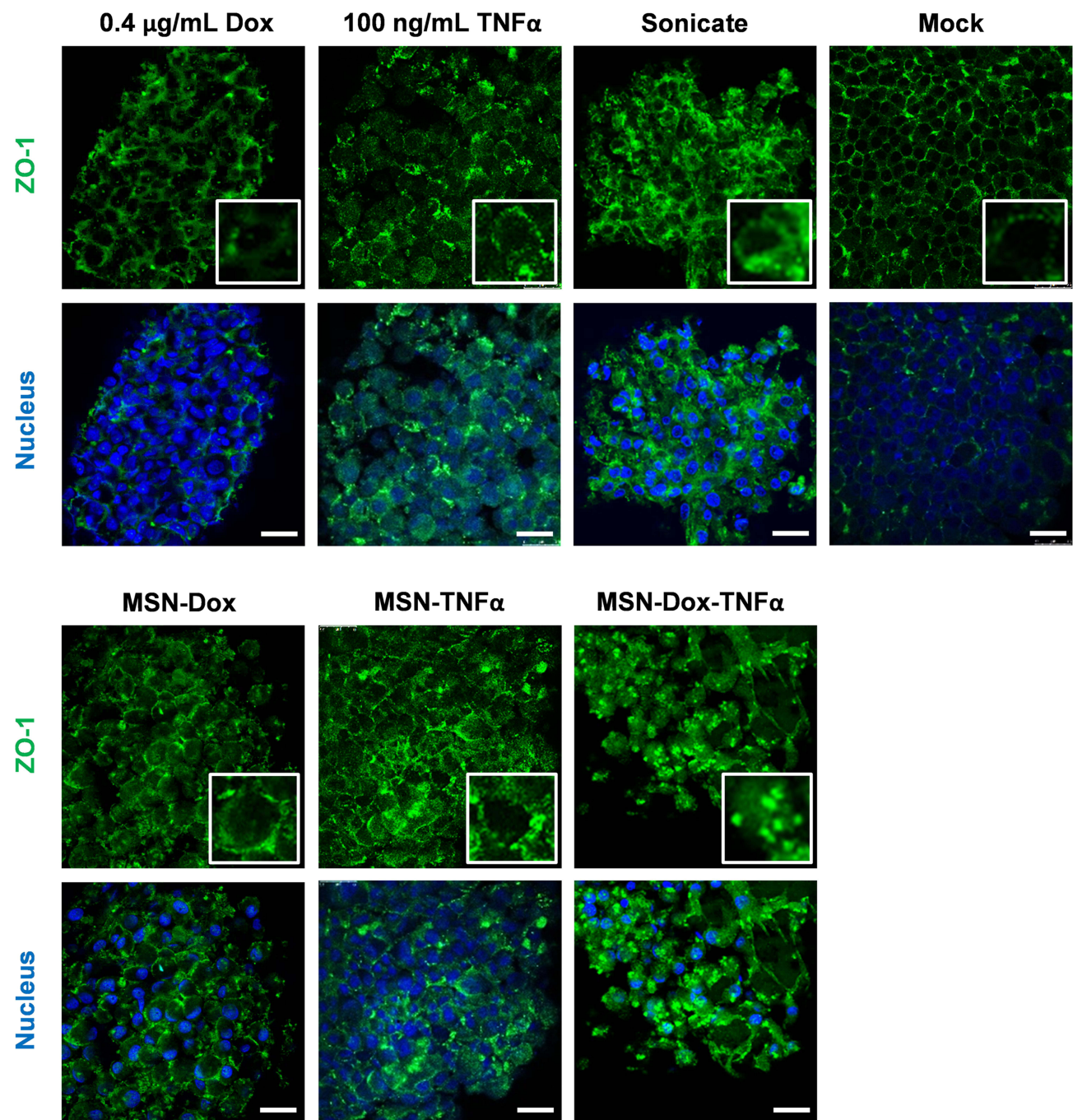


Figure 7 Tight junction staining (green) revealed an obvious effect of MSN-Dox-TNF α on 3D cell spheroids compared to free Dox or NP treatment. The sonicated cell spheroids as the positive control to mimic the leakage of the cell-cell tight junction. Scale bars: 25 μ m.

Abbreviations: ZO-1, Zonula occludens-1; MSN, mesoporous silica nanoparticles; Dox, doxorubicin; TNF α , tumor necrosis factor alpha; MSN-Dox, PEG-MSN-Hydrazone-Dox; MSN-TNF α , TNF α -PEG-MSN; MSN-Dox-TNF α , TNF α -PEG-MSN-Hydrazone-Dox.

relatively safe. Fluorescence histology examinations on tumor tissues isolated from various treatments for the expression of caspase-3 as the marker for apoptosis are shown in [Figure 8c](#). The strong fluorescence signals of activated caspase-3 denoting apoptosis were observed with MSN-Dox-TNF α treatment as compared to the control groups.

Different Concentration of TNF α Triggered Proliferation or Apoptosis in MES-SA/Dx5 Cells

Ki-67 is a nuclear protein that is used as a proliferation marker, unconstrained proliferation is one of the major features defining malignancy. Tumor cellular proliferative activity was determined as the ratio of Ki-67-positive cells measured

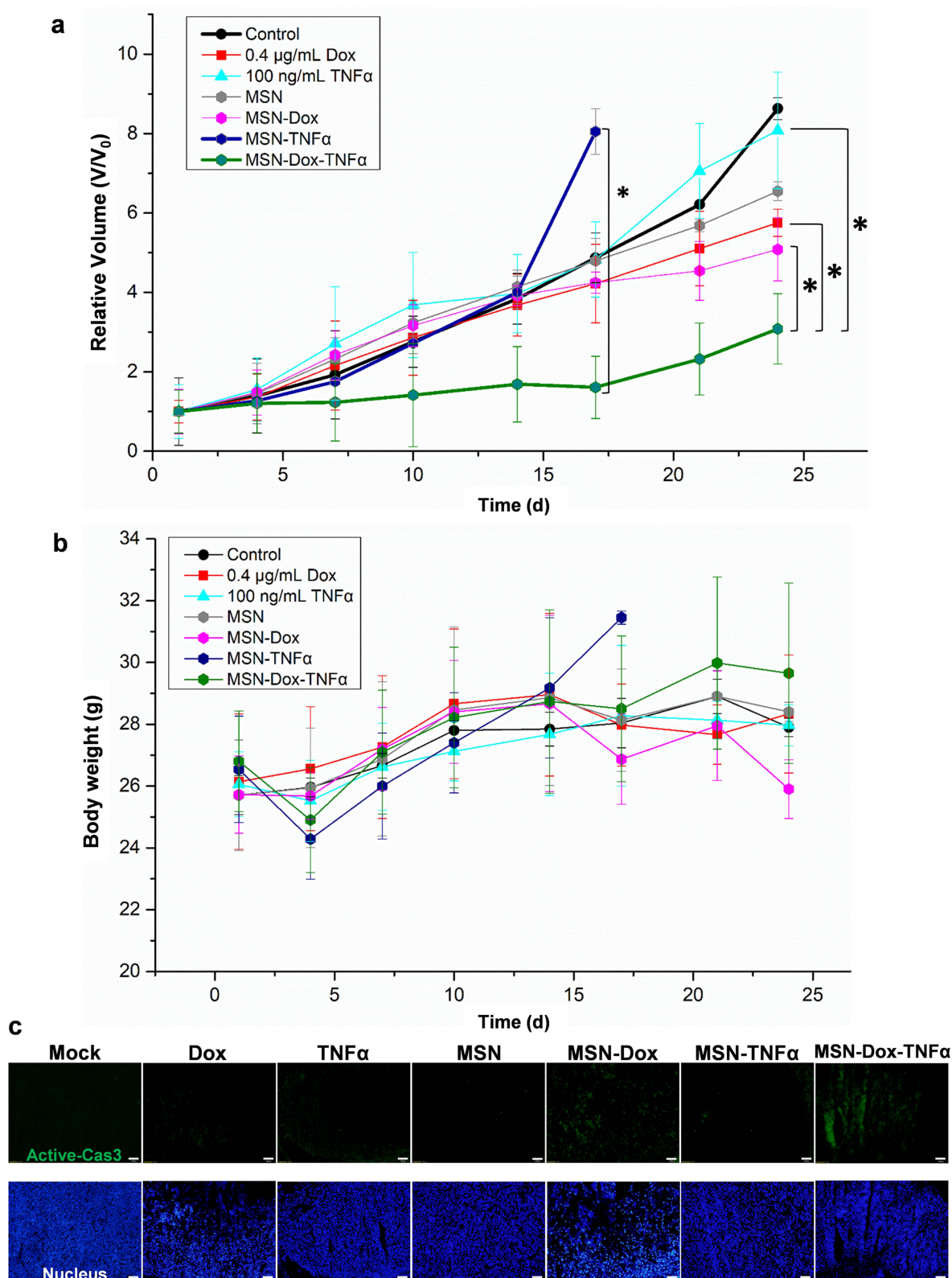


Figure 8 In vivo combination therapy effect of MSN-Dox-TNF α . MES-SA/Dx5 tumor-bearing mice were treated (i.t.) at Day 0 when the tumor volume reached 100 mm³ with MSN (50 μ g/mL), TNF α (100 ng/mL), Dox (0.4 μ g/mL), MSN-Dox, MSN-TNF α , and MSN-Dox-TNF α (50 μ g/mL). (a) Tumor volume and (b) body weight changes during the treatment. Data are the mean \pm SEM expressed as the fold-change of tumor volume relative to V₀. *P<0.05. (c) Immunofluorescence staining of activated caspase-3 expression (green) in tumor tissues after treatments. Scale bars: 100 μ m.

Abbreviations: MSN, mesoporous silica nanoparticles; Dox, doxorubicin; TNF α , tumor necrosis factor alpha; MSN-Dox, PEG-MSN-Hydrazone-Dox; MSN-TNF α , TNF α -PEG-MSN; MSN-Dox-TNF α , TNF α -PEG-MSN-Hydrazone-Dox.

by Ki-67 immunostaining.³⁰ After 6 h and 24 h post-treatment, cells were fixed and stained for Ki-67 and activated caspase-3. **Figure 9a** shows the distribution of Ki-67 (proliferation marker) and activated caspase-3 (apoptosis marker) in MES-SA/Dx5 cells incubated with formulations at 24 h post-treatment (h.p.t.). We also calculated the proliferation index and the percentages of activated caspase-3 positive cells at 6 h and 24 h post MSN-TNF α and MSN-Dox-TNF α treatments at various concentrations, as shown in **Figure 9b**. The results demonstrated that the proliferation index increased after the MSN-TNF α treatment, but not in a dose-dependent manner. The proliferation index indicated a 1.1-fold increase at 6 h.p.t. and a 1.5-fold increase at 24 h.p.t. The activated caspase-3 positive cell percentages, however, were significantly increased, while treated with high concentration of MSN-TNF α . These findings demonstrated that TNF α indeed triggered the proliferation pathway, even at a low concentration (as 10 $\mu\text{g}/\text{mL}$ MSN-TNF α is equal to 20 ng/mL of TNF α). Moreover, when the TNF α concentration was increased, an increasing number of cells also underwent the apoptosis pathway; however, the proliferation did not relatively increase as high as the apoptosis. We also treated the cells with 50 $\mu\text{g}/\text{mL}$ MSN-Dox-TNF α , which showed a combination therapy effect compared with the MSN-TNF α treatment group. As shown in **Figure 9c**, to further assess the critical concentration of TNF α dictating the contrary pathways of proliferation and apoptosis in vivo, MSN-TNF α was intratumorally administered in mice bearing MES-SA/Dx5 tumors with an amount of 50 $\mu\text{g}/\text{mL}$ and 250 $\mu\text{g}/\text{mL}$ (five folds higher dose). The standard concentration group illustrated the same proliferation pattern of tumor growth as that in **Figure 8a**. On the contrary, at the higher concentration of MSN-TNF α -treated mice, tumor growth was clearly inhibited. These results constitute evidence that, by varying dose, TNF α could play an opposite role in MES-SA/Dx5 cells.

Discussion

In this study, we showed that MSN-Dox-TNF α could be used effectively as a multifunctional drug delivery platform. First, the size of NP was smaller 100 nm, which is a suitable size for cell uptake,^{31,32} and PEG coating improved both dispersibility and macrophage uptake.^{33,34} TNF α provided an active targeting function to specifically accumulate in TNF α receptor over-expressed tumor cells. The TNF α -TNFR1 pathway not only subverts the drug-resistance mechanism in MES-SA/Dx5 cells, but also induces apoptosis by triggering the extrinsic apoptosis pathway. Dox is one of the most potent chemotherapeutic medications currently being used in clinical application, however it is still challenged by the development of MDR in cancer cells. It is dangerous to use Dox in drug resistant cancer cells because of concentration dependent toxicity to the heart pumping out the intracellular drug. The pH-sensitive MSN with two hydrazine bonds allowed Dox release in acidic environments, such as late endosome/lysosome, to enhance cytotoxicity in MES-SA/Dx5 cells by triggering intrinsic apoptosis pathway.³⁵ The enhanced apoptosis activity was due to reduced P-gp expression and increased cellular uptake of Dox by pH-controlled release to ensure a high intracellular drug concentration. Our MSN-Dox-TNF α can reduce P-gp expression by the TNF α -TNFR1 pathway, and the pH-controlled Dox release provides better anticancer activity than free drug at an equivalent Dox dosage. Not only the Dox, the delivery of Mitomycin C to MCF-7 (drug-sensitive) and MCF-7 KCR (MDR) cells via MSN, the increasing and possibly prolonged intracellular drug concentration which decreased the viability of both cells and the MCF-7 KCR shown obviously curing efficacy than free MMC treatments.³⁶ Combination therapy also proved effective to alleviate MDR. For instance, gold nanorods (Au NR) coated with gate keeper MSN loaded with Dox was used for combined chemo-photothermal therapy. Hairpin structure DNA as gate keeper released Dox in a controlled fashion followed by the laser irradiation subdued MDR and showed better antitumor therapeutic efficacy.³⁷

TNF α has long been of particular interest due to its multifunctional antitumor effects, which are apoptotic, antitumor immunotherapeutic response, and direct tumor cell lysis and proinflammatory pathways. In our study, we conjugated TNF α onto the surface of MSN for targeted delivery. TNF α simultaneously possesses targeting and therapeutic functions to enable a synergistic antitumor effect. Upon binding of the TNF α on the MSN, TNFR1 trimerizes, and the SODD protein is released.³⁸ Consequently, the adaptor proteins interact with key molecules that are responsible for downstream intracellular signaling.³⁹ This activation not only initiates a protease caspase, leading to apoptosis involving caspase as key regulators, but also down-regulates the expression of P-gp to deal with MDR.⁴⁰ A study showed that Dox-loaded Fe₃O₄ down-regulated the transcription of MDR-1 gene.⁴¹ A research group developed polyethyleneimine (PEI) -coated MSN to deliver both Dox and siRNA to inhibit the expression of P-gp, the results showed a better cytotoxic effect in

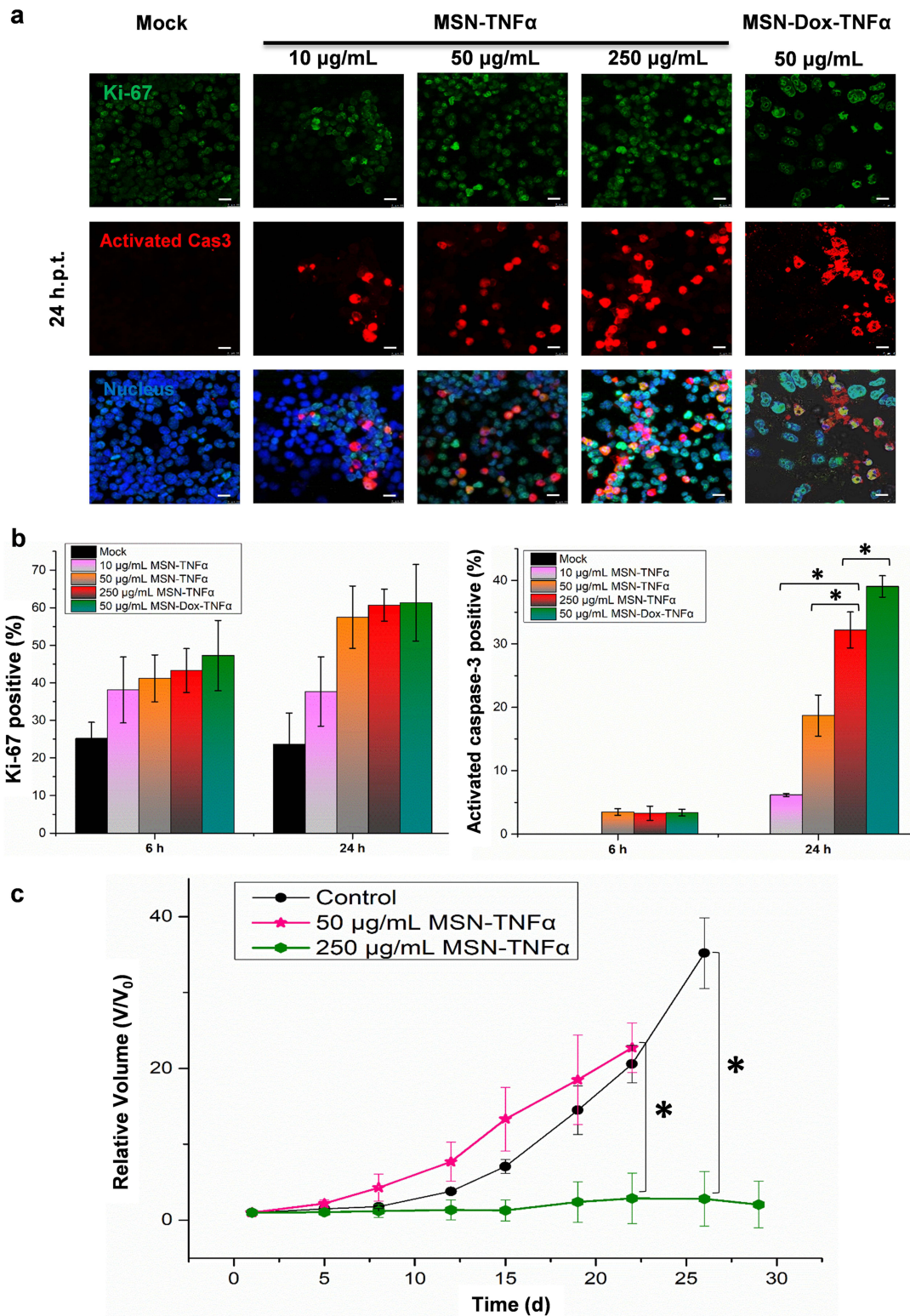


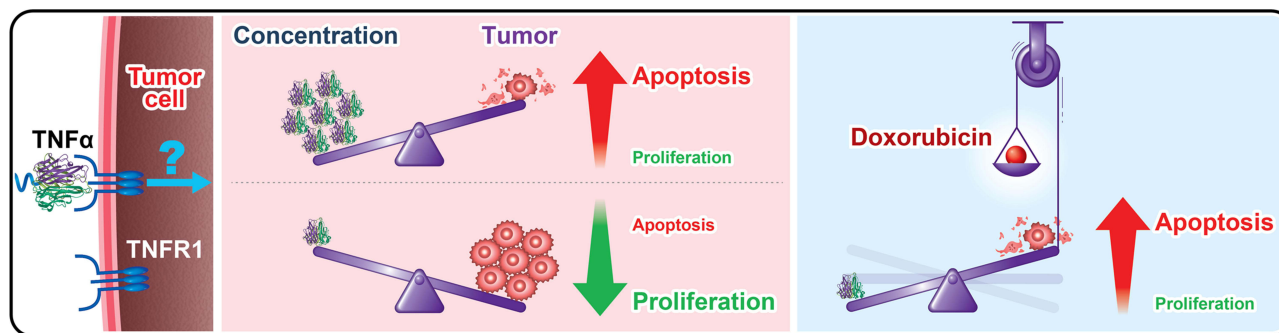
Figure 9 Double immunofluorescence staining of Ki-67 and activated caspase-3. After 6 and 24 h incubation, the MES-SA/Dx5 cells (1×10^6 cells/mL) were fixed and stained with DyLight 488 for Ki-67 (green), and DyLight 594 for activated caspase-3 (red). (a) Distribution of Ki-67 and activated caspase-3 in cells incubated with MSN-TNF α at 10, 50, or 250 μ g/mL, or MSN-Dox-TNF α at 50 μ g/mL. Scale bars: 10 μ m. (b) A percentage of Ki-67-positive cells or activated caspase-3 positive cells were fixed at 6 or 24 h post NP treatment. These were cumulative results of three independent experiments. Data are expressed as mean \pm SEM, *P<0.05. (c) Profiling of tumor growth in vivo under the treatments of MSN-TNF α at different concentrations. MES-SA/Dx5 tumor-bearing mice were treated (i.t.) at Day 0 when the tumor volume reached 100 mm³ with a standard dose of MSN-TNF α (50 μ g/mL) or a high dose of MSN-TNF α (250 μ g/mL). Data are the mean \pm SEM expressed as the fold-change of tumor volume relative to V₀. *P<0.05.

Abbreviations: MSN, mesoporous silica nanoparticles; Dox, doxorubicin; TNF α , tumor necrosis factor alpha; MSN-TNF α , TNF α -PEG-MSN; MSN-Dox-TNF α , TNF α -PEG-MSN-Hydrazone-Dox; h.p.t., hours post-treatment.

MDR cell line compared to free drug.⁴² Further, authors improved the co-deliver system by optimizing the ratio of Dox and siRNA with PEI-coated MSN that allowed synergistic tumor-killing efficacy with significant P-gp knockdown at heterogeneous tumor sites in vivo.⁴³ Wang et al used a similar idea and co-delivered Dox and siRNA to alleviate MDR in squamous carcinoma to achieve highly tumor-killing efficacy in vivo.⁴⁴ Researchers also demonstrated that Dox-loaded MSN could increase Dox accumulation and significantly reduce proliferation of MCF-7/ADR cells.⁴⁵ In our study, we found that MSN-TNF α inhibited P-gp expression by down-regulating protein expression levels by the TNF α -TNFR1 triggered pathway, which could explain why the enhanced chemotherapy efficacy of MSN-Dox against MES-SA/Dx5 cells that overexpress P-gp. The TNF α -TNFR1 pathway is also known to induce vascular damage and endothelial cell apoptosis, and triggers tumor cell apoptosis by the extrinsic pathway.⁴⁶

The inability of drugs to penetrate deeply into solid tumors is another critical challenge that conventional drug delivery systems could hardly overcome. To investigate the potential of MSN-Dox-TNF α to penetrate deeply into tumors, we observed the uptake and distribution of MSN-Dox-TNF α in a 3D tumor spheroids model. The results showed that more NP were accumulated and penetrated deeply in the tumor spheroids. This is because TNF α compromised the integrity of cell-cell tight junction proteins, which made them much leakier than untreated tumor spheroids. Other investigators showed patients with late stage cancers (Phase I clinical trials), that PEGylated colloidal 27-nm gold NP functionalized with TNF α (called CYT-6091) can increase the antitumor effects of chemotherapy and suppress tumor perfusion in murine models of mammary carcinoma when administered at doses of approximately 3–5 μ g of bioactive TNF α and combined with radiation therapy.⁴⁷ Recently, a study demonstrated obviously that lower doses (5–10 pg of bioactive TNF α) of iso1Au/TNF α are enough to influence antitumor efficacy and vascular permeability of chemotherapy. Indeed, the markedly low dose of TNF α constitutes a significant advantage in terms of toxicity.⁴⁸ Our MSN-Dox-TNF α was conjugated with a higher TNF α concentration, but exhibited negligible cytotoxicity to normal cells and induced synergistic therapeutic effects with the pH-controlled release of Dox. Cytimmune[®] also developed several promising second-generation candidates that carry several therapeutic agents on the same 27-nm gold NP in preclinical studies, such as paclitaxel or Dox.⁴⁹ In the future, our MSN-Dox-TNF α is a potential candidate for translation in preclinical settings.

In our study, we also found another interesting result regarding TNF α treatment concentration. It is well known that TNF α acts as a multifunctional cytokine with many different functions by triggering signaling pathways, such as JNK (c-Jun N-terminal kinase) and NF- κ B (nuclear factor kappa-light-chain-enhancer of activated B cells). Activation of JNK by TNF α is mediated by the recruitment of adaptor proteins, such as TRADD (TNF receptor-associated death domain) and FADD (Fas-associated death domain), to the TNF receptor. Whereas, activation of NF- κ B by TNF α involves the recruitment of a complex of proteins, including TRAF2 (TNF receptor-associated factor 2) and RIP1 (receptor-interacting protein 1), to the TNF receptor. The fate of cells in response to TNF α -induced activation of JNK and NF- κ B signaling pathways is complex and can have diverse outcomes depending on the cellular context.⁵⁰ TNF α induced antitumor effects, which included antitumor immunotherapeutic response through apoptotic and direct tumor cell lysis and proinflammatory pathways. As a consequence, TNF α could be a molecular objective for cancer treatment. The antitumor immune modulation properties had already achieved promising efficacy when used locally. However, TNF α -induced systematic toxicity substantially diminishes potential for its application in clinical settings. For this reason, it is a good strategy to incorporate TNF α in a nano delivery system which can reduce its systemic toxicity and target tumors. In our in vivo experiment, we discovered that when treated with MSN-TNF α alone (equivalent to 100 ng/mL of TNF α) tumor size increased after 7 d post-treatment (compared with MSN-Dox-TNF α and mock groups), while MSN-Dox-TNF α treatment showed a significant tumor inhibition effect. From this result, it could be concluded that TNF α plays a dual role of proliferation and apoptosis activity controlled by its concentration. Even some research groups observed the proliferation of human nucleus pulposus cells by escalating dose of TNF α (20–80 ng/mL), which favored the activation of NF- κ B and MAPK signaling by promotes by.⁵¹ But in the higher concentration of TNF α , such proliferation and signaling activation were not observed (80–120 ng/mL around 40% Ki-67 positive cells). To further confirm this, we treated the tumor with different concentrations of MSN-TNF α in order to evaluate the tumor-killing efficacy. Tumor growth was inhibited strongly under a five-fold higher dose of TNF α (equivalent to approximately 500 ng/mL of TNF α). On the contrary, at a lower concentration (equivalent to approximately 100 ng/mL of TNF α), the tumor volume increased by several folds. It implicates that the concentration of TNF α is a crucial factor for tumors to undergo either proliferation or apoptosis pathways (Scheme 2).



Scheme 2 Schematic illustration of the concentration-dependent bi-functional effect of $\text{TNF}\alpha$ in the modulation of proliferation and apoptosis in vivo. The combination of Dox and $\text{TNF}\alpha$ could significantly inhibit tumor growth via both intrinsic and extrinsic apoptosis pathways.

Abbreviations: $\text{TNF}\alpha$, tumor necrosis factor alpha; TNFR1, TNF receptor type 1.

Conclusion

We synthesized $\text{TNF}\alpha$ -conjugated pH-responsive MSN that down-regulated the expression level of P-gp, facilitating the targeted uptake in drug-resistant cancer cells. Intracellular release of Dox through cleavage of hydrazone bonds resulted in its abundant accumulation, which significantly reduced cell viability via both intrinsic and extrinsic apoptosis pathways. In a 3D tumor spheroid model, our nanoplatform demonstrated the deep penetration achieved by the $\text{TNF}\alpha$ -induced disintegration of tight junction proteins. In the in-vivo study, the MSN-Dox- $\text{TNF}\alpha$ harnessing both intrinsic and extrinsic apoptosis pathways effectively inhibited tumor growth in a synergistic manner of Dox and $\text{TNF}\alpha$. Of particular interest, the in-vivo analysis further indicated that the concentration of MSN- $\text{TNF}\alpha$ is a crucial factor determining tumors to undergo either proliferation or apoptosis, two pathways in opposite directions.

Abbreviations

MDR, multidrug resistance; Dox, doxorubicin; $\text{TNF}\alpha$, tumor necrosis factor alpha; NP, Nanoparticles; MSN, mesoporous silica nanoparticles; Fourier transform infrared, FTIR; Polydispersity, PDI; P-gp, p-glycoprotein; PEG, polyethylene glycol; MSN-Dox, PEG-MSN-Hydrazone-Dox; MSN-Dox- $\text{TNF}\alpha$, $\text{TNF}\alpha$ -PEG-MSN-Hydrazone-Dox; CI, combination index; NK, natural killer; TNFR1, TNF receptor type 1, p55; TNFR2, TNF receptor type 2, p75; EPR, enhanced permeability and retention; mAb, monoclonal antibody; ZO-1, Zonula occludens-1; JNK, c-Jun N-terminal kinase; NF- κ B, nuclear factor κ B; h.p.t., hours post-treatment.

Data Sharing Statement

All data generated or analyzed during this study are included in this manuscript.

Ethics Approval and Consent to Participate

The animal study was reviewed and approved by the Institutional Animal Care and Use Committee of the National Health Research Institutes (Taiwan).

Consent for Publication

All authors agreed to publish the final manuscript.

Acknowledgments

This study was supported by the grants BN-110-PP-04 and NHRI-EX110-10829EI from National Health Research Institutes of Taiwan, and MOST 110-2112-M-400-001 from the Ministry of Science and Technology of Taiwan. We also thank core facility center of NHRI to provide confocal microscope imaging system service. We truly appreciate Ms Hsin-Ying Huang for her great assistance on TEM imaging analysis (IBEN services, National Health Insurance Research, Taiwan).

Author Contributions

All authors made a significant contribution to the work reported, whether that is in the conception, study design, execution, acquisition of data, analysis and interpretation, or in all these areas; took part in drafting, revising or critically reviewing the article; gave final approval of the version to be published; have agreed on the journal to which the article has been submitted; and agree to be accountable for all aspects of the work.

Funding

This study was supported by the grants BN-110-PP-04 and NHRI-EX110-10829EI from National Health Research Institutes of Taiwan, and MOST 110-2112-M-400-001 from the Ministry of Science and Technology of Taiwan.

Disclosure

The authors have declared that no competing interest exists in this work.

References

1. Berraondo P, Sanmamed MF, Ochoa MC, et al. Cytokines in clinical cancer immunotherapy. *Br J Cancer*. 2019;120:6–15. doi:10.1038/s41416-018-0328-y
2. Young PA, Morrison SL, Timmerman JM. Antibody-cytokine fusion proteins for treatment of cancer: engineering cytokines for improved efficacy and safety. *Semin Oncol*. 2014;41:623–636. doi:10.1053/j.seminoncol.2014.08.002
3. Kontermann RE. Antibody–cytokine fusion proteins. *Arch Biochem Biophys*. 2012;526:194–205. doi:10.1016/j.abb.2012.03.001
4. Johansson A, Hamzah J, Payne CJ, Ganss R. Tumor-targeted TNF α ; stabilizes tumor vessels and enhances active immunotherapy. *PNAS*. 2012;109:7841–7846. doi:10.1073/pnas.1118296109
5. Pasche N, Neri D. Immunocytokines: a novel class of potent armed antibodies. *Drug Discov Today*. 2012;17:583–590. doi:10.1016/j.drudis.2012.01.007
6. Vivero-Escoto JL, Slowing II, Trewyn BG, Lin VSY. Mesoporous silica nanoparticles for intracellular controlled drug delivery. *Small*. 2010;6:1952–1967. doi:10.1002/smll.200901789
7. Gaur U, Aggarwal BB. Regulation of proliferation, survival and apoptosis by members of the TNF superfamily. *Biochem Pharmacol*. 2003;66:1403–1408. doi:10.1016/S0006-2952(03)00490-8
8. Wajant H, Pfizenmaier K, Scheurich P. Tumor necrosis factor signaling. *Cell Death Differ*. 2003;10:45–65. doi:10.1038/sj.cdd.4401189
9. Ashkenazi A, Dixit VM. Death receptors: signaling and modulation. *Science*. 1998;281:1305–1308. doi:10.1126/science.281.5381.1305
10. van Horsen R, Ten Hagen TL, Eggermont AM. TNF-alpha in cancer treatment: molecular insights, antitumor effects, and clinical utility. *Oncologist*. 2006;11:397–408. doi:10.1634/theoncologist.11-4-397
11. Boland K, Flanagan L, Prehn J. Paracrine control of tissue regeneration and cell proliferation by Caspase-3. *Cell Death Dis*. 2013;4:e725. doi:10.1038/cddis.2013.250
12. Chapman PB, Lester TJ, Casper ES, et al. Clinical pharmacology of recombinant human tumor necrosis factor in patients with advanced cancer. *J Clin Oncol*. 1987;5:1942–1951. doi:10.1200/JCO.1987.5.12.1942
13. Jakubowski AA, Casper ES, Gabrilove JL, Templeton MA, Sherwin SA, Oettgen HF. Phase I trial of intramuscularly administered tumor necrosis factor in patients with advanced cancer. *J Clin Oncol*. 1989;7:298–303. doi:10.1200/JCO.1989.7.3.298
14. Kedar E, Palgi O, Golod G, Babai I, Barenholz Y. Delivery of cytokines by liposomes. III. Liposome-encapsulated GM-CSF and TNF-alpha show improved pharmacokinetics and biological activity and reduced toxicity in mice. *J Immunother*. 1997;20:180–193. doi:10.1097/00002371-199705000-00003
15. van der Veen AH, Eggermont AMM, Seynhaeve ALB, van Tiel ST, ten Hagen TLM. Biodistribution and tumor localization of stealth liposomal tumor necrosis factor- α in soft tissue sarcoma bearing rats. *Int J Cancer*. 1998;77:901–906. doi:10.1002/(SICI)1097-0215(19980911)77:6
16. Sheno MM, Iltis I, Choi J, et al. Nanoparticle Delivered Vascular Disrupting Agents (VDAs): use of TNF-alpha conjugated gold nanoparticles for multimodal cancer therapy. *Mol Pharm*. 2013;10:1683–1694. doi:10.1021/mp300505w
17. Libutti SK, Paciotti GF, Byrnes AA, et al. Phase I and pharmacokinetic studies of CYT-6091, a novel PEGylated colloidal gold-rhTNF nanomedicine. *Clin Cancer Res*. 2010;16:6139–6149. doi:10.1158/1078-0432.CCR-10-0978
18. Paciotti GF, Myer L, Weinreich D, et al. Colloidal gold: a novel nanoparticle vector for tumor directed drug delivery. *Drug Deliv*. 2004;11:169–183. doi:10.1080/10717540490433895
19. Shao J, Griffin RJ, Galanzha EI, et al. Photothermal nanodrugs: potential of TNF-gold nanospheres for cancer theranostics. *Sci Rep*. 2013;3:1293. doi:10.1038/srep01293
20. Xu G, Gu H, Hu B, et al. PEG-b-(PELG-g-PLL) nanoparticles as TNF- α nanocarriers: potential cerebral ischemia/reperfusion injury therapeutic applications. *Int J Nanomed*. 2017;12:2243–2254. doi:10.2147/IJN.S130842
21. Lee C-H, Cheng S-H, Wang Y-J, et al. Near-infrared mesoporous silica nanoparticles for optical imaging: characterization and in vivo biodistribution. *Adv Funct Mater*. 2009;19:215–222. doi:10.1002/adfm.200800753
22. Chen NT, Souris JS, Cheng SH, et al. Lectin-functionalized mesoporous silica nanoparticles for endoscopic detection of premalignant colonic lesions. *Nanomedicine*. 2017;13:1941–1952. doi:10.1016/j.nano.2017.03.014
23. Jafari S, Derakhshankhah H, Alaei L, Fattahi A, Varnamkhasi BS, Saboury AA. Mesoporous silica nanoparticles for therapeutic/diagnostic applications. *Bio Pharmacol*. 2019;109:1100–1111. doi:10.1016/j.biopha.2018.10.167
24. Lee C-H, Cheng S-H, Huang I-P, et al. Intracellular pH-responsive mesoporous silica nanoparticles for the controlled release of anticancer chemotherapeutics. *Angew Chem Int Ed*. 2010;49:8214–8219. doi:10.1002/anie.201002639

25. Zhou Y, Quan G, Wu Q, et al. Mesoporous silica nanoparticles for drug and gene delivery. *Acta Pharm Sin B*. 2018;8:165–177. doi:10.1016/j.apsb.2018.01.007
26. Cheng S-H, Lee C-H, Chen M-C, et al. Tri-functionalization of mesoporous silica nanoparticles for comprehensive cancer theranostics—the trio of imaging, targeting and therapy. *J Mater Chem*. 2010;20:6149–6157. doi:10.1039/c0jm00645a
27. Lu J, Liang M, Li Z, Zink JI, Tamanoi F. Biocompatibility, biodistribution, and drug-delivery efficiency of mesoporous silica nanoparticles for cancer therapy in animals. *Small*. 2010;6:1794–1805. doi:10.1002/sml.201000538
28. Tsai C-P, Chen C-Y, Hung Y, Chang F-H, Mou C-Y. Monoclonal antibody-functionalized mesoporous silica nanoparticles (MSN) for selective targeting breast cancer cells. *J Mater Chem*. 2009;19:5737–5743. doi:10.1039/B905158A
29. Stevenson BR, Siliciano JD, Mooseker MS, Goodenough DA. Identification of ZO-1: a high molecular weight polypeptide associated with the tight junction (zonula occludens) in a variety of epithelia. *J Cell Biol*. 1986;103:755–766. doi:10.1083/jcb.103.3.755
30. Scholzen T, Gerdes J. The Ki-67 protein: from the known and the unknown. *J Cell Physiol*. 2000;182:311–322. doi:10.1002/(SICI)1097-4652(200003)182:3
31. Foroozandeh P, Aziz AA. Insight into cellular uptake and intracellular trafficking of nanoparticles. *Nanoscale Res Lett*. 2018;13:339. doi:10.1186/s11671-018-2728-6
32. Haddick L, Zhang W, Reinhard S, et al. Particle-size-dependent delivery of antitumoral miRNA using targeted mesoporous silica nanoparticles. *Pharmaceutics*. 2020;12(6):505. doi:10.3390/pharmaceutics12060505
33. Ravi Kumar MN. Nano and microparticles as controlled drug delivery devices. *J Pharm Pharm Sci*. 2000;3:234–258.
34. Walkey CD, Olsen JB, Guo H, Emili A, Chan WCW. Nanoparticle size and surface chemistry determine serum protein adsorption and macrophage uptake. *J Am Chem Soc*. 2012;134:2139–2147. doi:10.1021/ja2084338
35. Huang I-P, Sun S-P, Cheng S-H, et al. Enhanced chemotherapy of cancer using pH-sensitive mesoporous silica nanoparticles to antagonize P-glycoprotein-mediated drug resistance. *Mol Cancer Ther*. 2011;10:761–769. doi:10.1158/1535-7163.MCT-10-0884
36. Igaz N, Béltéky P, Kovács D, et al. Functionalized mesoporous silica nanoparticles for drug-delivery to multidrug-resistant cancer cells. *Int J Nanomed*. 2022;17:3079–3096. doi:10.2147/IJN.S363952
37. Yang X, Li M, Liang JI, Hou XY, He XX, Wang KM. NIR-controlled treatment of multidrug-resistant tumor cells by mesoporous silica capsules containing gold nanorods and doxorubicin. *ACS Appl Mater Interfaces*. 2021;13(13):14894–14910. doi:10.1021/acsami.0c23073
38. Takada H, Chen NJ, Mirtsos C, et al. Role of SODD in regulation of tumor necrosis factor responses. *Mol Cell Biol*. 2003;23:4026–4033. doi:10.1128/MCB.23.11.4026-4033.2003
39. MacEwan DJ. TNF ligands and receptors—a matter of life and death. *Br J Pharmacol*. 2002;135:855–875. doi:10.1038/sj.bjp.0704549
40. Walther W, Kobelt D, Bauer L, Aumann J, Stein U. Chemosensitization by diverging modulation by short-term and long-term TNF- α action on ABCB1 expression and NF- κ B signaling in colon cancer. *Int J Oncol*. 2015;47(6):2276–2285. doi:10.3892/ijo.2015.3189
41. Bu H, Gao Y, Li Y. Overcoming multidrug resistance (MDR) in cancer by nanotechnology. *Sci China Chem*. 2010;53:2226–2232. doi:10.1007/s11426-010-4142-5
42. Meng H, Liang M, Xia T. Engineered design of mesoporous silica nanoparticles to deliver doxorubicin and P-glycoprotein siRNA to overcome drug resistance in a cancer cell line. *ACS nano*. 2010;4(8):4539–4550. doi:10.1021/nn100690m
43. Meng H, Mai W, Zhang H. Codelivery of an optimal drug/siRNA combination using mesoporous silica nanoparticles to overcome drug resistance in breast cancer in vitro and in vivo. *ACS nano*. 2013;7(2):994–1005. doi:10.1021/nn3044066
44. Wang D, Xu X, Zhang K. Codelivery of doxorubicin and MDR1-siRNA by mesoporous silica nanoparticles-polymerpolyethylenimine to improve oral squamous carcinoma treatment. *Int J Nanomed*. 2018;13:187–198. doi:10.2147/IJN.S150610
45. Shen J, He Q, Gao Y, Shi J, Li Y. Mesoporous silica nanoparticles loading doxorubicin reverse multidrug resistance: performance and mechanism. *Nanoscale*. 2011;3:4314–4322. doi:10.1039/C1NR10580A
46. Ashkenazi A, Dixit VM. Apoptosis control by death and decoy receptors. *Curr Opin Cell Biol*. 1999;11:255–260. doi:10.1016/S0955-0674(99)80034-9
47. Koonce N, Quick C, Hardee M, et al. Combination of gold nanoparticle-conjugated tumor necrosis factor- α and radiation therapy results in a synergistic antitumor response in murine carcinoma models. *IJROBP*. 2015;93:588–596. doi:10.1016/j.ijrobp.2015.07.2275
48. Corti A, Sacchi A, Gasparri AM, et al. Enhancement of doxorubicin anti-cancer activity by vascular targeting using IsoDGR/cytokine-coated nanogold. *J Nanobiotechnol*. 2021;19:128. doi:10.1186/s12951-021-00871-y
49. Evans ER, Bugga P, Asthana V, Drezek R. Metallic nanoparticles for cancer immunotherapy. *Mater Today*. 2018;21:673–685. doi:10.1016/j.mattod.2017.11.022
50. Papa S, Zazzeroni F, Pham CG, Bubici C, Franzoso G. Linking JNK signaling to NF- κ B: a key to survival. *J Cell Sci*. 2004;117:5197–5208. doi:10.1242/jcs.01483
51. Wang X-H, Hong X, Zhu L, et al. Tumor necrosis factor alpha promotes the proliferation of human nucleus pulposus cells via nuclear factor- κ B, c-Jun N-terminal kinase, and p38 mitogen-activated protein kinase. *Exp Biol Med*. 2015;240:411–417. doi:10.1177/1535370214554533

International Journal of Nanomedicine

Dovepress

Publish your work in this journal

The International Journal of Nanomedicine is an international, peer-reviewed journal focusing on the application of nanotechnology in diagnostics, therapeutics, and drug delivery systems throughout the biomedical field. This journal is indexed on PubMed Central, MedLine, CAS, SciSearch®, Current Contents®/Clinical Medicine, Journal Citation Reports/Science Edition, EMBASE, Scopus and the Elsevier Bibliographic databases. The manuscript management system is completely online and includes a very quick and fair peer-review system, which is all easy to use. Visit <http://www.dovepress.com/testimonials.php> to read real quotes from published authors.

Submit your manuscript here: <https://www.dovepress.com/international-journal-of-nanomedicine-journal>